Publication № 1

polymers

MDPI

Article

Additive Effects on Phase Transition and Interactions in Poly(vinyl methyl ether) Solutions

Larisa Starovoytova [1], Julie Šťastná [2], Adriana Šturcová [3], Rafal Konefal [1], Jiří Dybal [3], Nadiia Velychkivska [1], Marek Radecki [2] and Lenka Hanyková [2,*]

Received: 27 August 2015; Accepted: 30 November 2015; Published: 4 December 2015
Academic Editor: Richard Hoogenboom

[1] Department of NMR Spectroscopy, Institute of Macromolecular Chemistry AS CR, v.v.i., Heyrovského Sq. 2, 162 06 Prague, Czech Republic; larisa@imc.cas.cz (L.S.); konefal.rafal@gmail.com (R.K.); velychkivska@imc.cas.cz (N.V.)
[2] Department of Macromolecular Physics, Faculty of Mathematics and Physics, Charles University in Prague, V Holešovičkách 2, 180 00 Prague 8, Czech Republic; chamky@seznam.cz (J.Š.); radecki.m@seznam.cz (M.R.)
[3] Department of Vibrational Spectroscopy, Institute of Macromolecular Chemistry AS CR, v.v.i., Heyrovského Sq. 2, 162 06 Prague, Czech Republic; sturcova@imc.cas.cz (A.Š.); dybal@imc.cas.cz (J.D.)
* Correspondence: Lenka.Hanykova@mff.cuni.cz; Tel.: +420-2-2191-2368; Fax: +420-2-2191-2350

Abstract: A comparative study of thermal response of poly(vinyl methyl ether) in the presence of different hydrophilic and hydrophobic additives was performed by Nuclear magnetic resonance (NMR) spectroscopy, Fourier-transform infrared (FTIR) spectroscopy, differential scanning calorimetry (DSC), and optical microscopy. The effect of polymer concentration and additive content on the appearance and extent of the phase transition was determined. A detailed study of interaction mechanism in solutions with two hydrophobic additives showed differences in the way in which polymer globules are formed. For solutions containing *t*-butyl methyl ketone and *t*-butanol, measurements of ^{1}H spin-spin relaxations showed the presence of water and additive molecules bound in PVME globular structures. These originally-bound molecules are then slowly released from the globular-like structures. Incorporation of molecules into the globules disrupts the cooperativity of the transition and affects the size of globular structures.

Keywords: additives; LCST; poly(vinyl methyl ether); thermal properties

1. Introduction

The applications of stimuli-responsive polymers are becoming more and more diversified. The ability of the polymers to change their behavior according to external conditions, and the possibility to moderate this effect, make such systems interesting for drug delivery applications, as sensors, and in cosmetics [1–4]. Investigations of the transition phenomena in model systems can offer knowledge that is of practical use. Poly(vinyl methyl ether) (PVME) is a non-ionic water-soluble polymer with useful properties, such as biocompatibility, non-toxicity, low glass transition temperature and thermoresponsive behavior with lower critical solution temperature (LCST) around 308 K [5–7]. The phase transition effects for this polymer have been widely investigated by different experimental techniques, such as differential scanning calorimetry (DSC) [8–10], Nuclear magnetic resonance (NMR) spectroscopy [11,12], and Fourier-transform infrared (FTIR) spectroscopy [6,13,14].

Modification of the transition conditions (such as the transition temperature) of thermoresponsive polymers can be achieved in different ways, such as variation of the hydrophobicity of the polymer chain by copolymerization with hydrophobic or hydrophilic co-monomers or changes in the composition of the solvent by mixing the aqueous polymer solution with small molecules (additives) that alter the polymer-water interaction [15–18].

Additive molecules can sometimes be used as a crude model of a medical drug for examining drug delivery systems [19,20]. The ability of an additive compound to interact with the polymer chain on the one hand and to bind water molecules on the other hand plays an important role in its influence on the transition mechanism [11]. In particular, the ability of the additive to be embedded into the polymer globules affects the mechanism of their formation and the kinetics of water release and, possibly, also the additive release from the globular structures. Based on their influence on polymer structure, it is possible to distinguish two types of additives, namely those that either stabilize or destabilize the hydration structure surrounding the polymer chain [21].

In previous studies of similar systems, it was found that even a small amount of an additive can change the transition temperature and the mechanism of the phase separation in PVME solutions. For example, although propanol has almost no effect on this polymer behavior, lower molecular weight alcohols are able to relatively stabilize the polymer structure, whereas higher alcohols and simple inorganic salts tend to destabilize the structure, *i.e.*, lead to lower transition temperatures [18,22].

In this work we perform a comparative analysis of the phase separation of PVME in the presence of structurally similar additives, *t*-butyl methyl ketone (TBMK), *t*-butyl methyl ether (TBME), *t*-butylamine (TBAm), and *t*-butanol (TBOH) differing in individual chemical groups (carbonyl, ether, amine, and hydroxyl group, respectively). Several experimental techniques were used in this investigation. NMR and FTIR were used to individually analyze the additive, water, and polymer segments and analyze their mobility and interactions during the transition. DSC and optical microscopy were used to characterize the macroscopic behavior of the sample as a whole. Differences in the mechanism of transition because of the presence of these additives are discussed.

2. Experimental Section

2.1. Materials

PVME was purchased from Sigma-Aldrich (St. Louis, MO, USA) and was supplied as 50 wt % aqueous solution (molecular weight determined by SEC in THF was M_w = 60,500, $M_w/M_n \approx 3$). *t*-Butyl methyl ketone, *t*-butyl methyl ether, *t*-butylamine, and *t*-butanol (see Figure 1 for the structures) were purchased from Sigma-Aldrich (St. Louis, MO, USA) and were used as obtained. After drying, the polymer was used to prepare PVME in D_2O (99.96% of deuterium) solutions with polymer concentrations c_P = 0.5−10 wt % and concentrations of additives c_{ad} = 0−10 wt %. All the PVME/D_2O samples in 5 mm NMR tubes were degassed and were sealed under argon; sodium 2,2-dimethyl-2-silapentane-5-sulfonate (DSS) was used as an internal NMR standard.

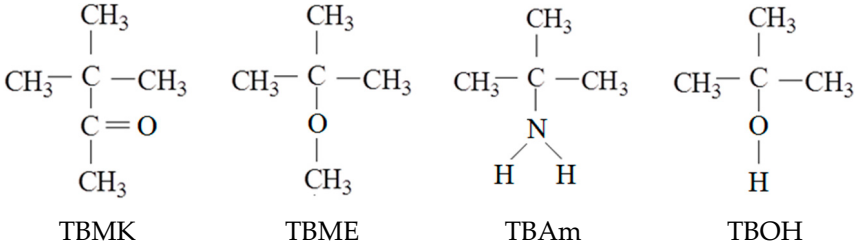

Figure 1. Structural formulae of *t*-butyl methyl ketone (TBMK); *t*-butyl methyl ether (TBME); *t*-butylamine (TBAm); and *t*-butanol (TBOH).

2.2. NMR Mesurements

^{1}H NMR spectra were measured with a Bruker 600 MHz Avance III spectrometer (Billerica, MA, USA, 5 mm NMR tubes were used). The integrated signal intensities were determined with the spectrometer integration software with an accuracy of ±1%. The temperature was kept constant within ±0.2 K with a BVT 3000 temperature unit. The typical measurement conditions for ^{1}H were as follows: a spectral width of 6 kHz, a pulse width of 10 μs (90° pulse) and a relaxation

delay of 20 s. The ^{1}H spin-spin relaxation times T_2 were measured with the CPMG pulse sequence 90°_x-(t_d-180°_x-t_d)$_n$-acquisition, for t_d = 0.5 ms.

2.3. Infrared Spectroscopy

Attenuated total reflectance (ATR) FTIR spectra of the PVME solution, neat PVME (containing a small amount of absorbed water), TBME, and TBMK solutions were collected with a Nicolet Nexus 870 FTIR spectrometer (Thermo Fisher Scientific, Waltham, MA, USA) purged with dry air and equipped with a cooled mercury-cadmium-telluride (MCT) detector. The samples were measured on a horizontal ATR Golden Gate unit (SPECAC Ltd., Orpington, UK) with a diamond prism and a controlled heated top plate; the spectral resolution was 4 cm^{-1}. All the spectra were processed with the advanced ATR correction with OMNIC^{TM} software (Thermo Fisher Scientific, Waltham, MA, USA). The spectrum of neat D_2O at the corresponding temperature was subtracted to better visualize the dissolved compounds. In addition, the spectrum of PVME at the corresponding temperature was subtracted from spectra in Figure 8d,e to visualize the TBME additive only; this subtraction is responsible for the baseline distortion. The spectra were scaled.

2.4. DSC

DSC measurements were performed with a differential scanning calorimeter, Pyris 1 (Perkin-Elmer, Waltham, MA, USA); two complete cycles with heating and cooling rates of 5 K· min^{-1} over a range of 275–325 K were performed. Samples of approximately 10 mg were encapsulated in aluminum pans. The transition was characterized by calculation of the enthalpy changes per unit mass of PVME through integration of the experimental DSC thermograms.

2.5. Optical Microscopy

Optical microscope measurements were carried out under nitrogen atmosphere with a Nikon Eclipse 80i (Nikon Instruments, Amsterdam, Netherlands); a camera, PixeLINK PL-A662 (PixeLINK, Ottawa, ON, Canada); and a temperature cell, Linkam LTS350 (Linkam Scientific Instruments, Surrey, UK). Development of the morphology was observed for a thin sample layer placed between a support glass slide and a cover slip, with 50-fold magnification. The heating rate was 1 K· min^{-1}, and before each experiment, the samples were always maintained at the experimental temperature for 1 min.

3. Results and Discussion

3.1. Influence of Additives on the Phase Transition

The intensity and shape of the polymer, additive, and water HDO signals in NMR spectra vary with temperature. The polymer signal vanishes from the high-resolution NMR spectra because of broadening (often extreme) of the polymer peak due to the restriction in the mobility of polymer chains upon formation of the solid-like globules [5,11]. Figure 2 shows ^{1}H NMR spectra as detected for the neat PVME solution and solutions of PVME with additives at temperatures above the transition of each particular system. The shapes of the peaks in the spectra are different for individual additives and for the pure PVME solution.

We can distinguish two types of polymer peaks [5]. The first type corresponds to flexible polymer segments which are not involved in compact globular structures (the narrow part of the CH_3O peak at 3.5 ppm in spectrum a, Figure 2). The second type is assigned to the major part of polymer units which form solid-like globular structures (the broad part of the same peak from 4 to 5 ppm). The presence of additives strongly affects the shape of both polymer band components. As shown in Figure 2, the signal of the units in globular structures is extremely broadened, so it is no longer visible in the spectra (spectra in Figure 2b–e); this disappearance suggests that the polymer units involved in globules formed in solutions with additives show higher immobilization in comparison with collapsed units in the solution of neat PVME. Further, it follows from Figure 2 that the shape of NMR signal

corresponding to PVME group $CHOCH_3$ depends on the additive. The solution with TBME shows quite narrow $CHOCH_3$ peak whereas, for solutions with others additives, this peak broadens.

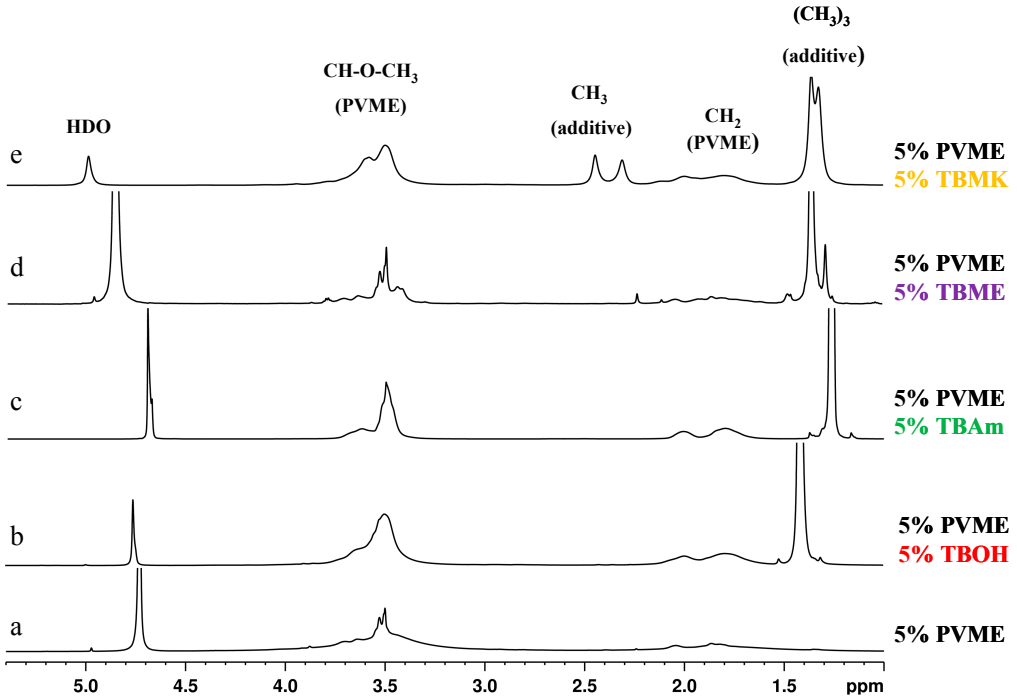

Figure 2. High-resolution ^{1}H NMR spectra of D_2O solutions of neat PVME (c_P = 5 wt %) (**a**); and solutions with additives TBOH (**b**); TBAm (**c**); TBME (**d**); and TBMK (**e**) (c_P = 5 wt %, c_{ad} = 5 wt %) measured at temperatures above the transition of each particular system.

For further analysis, we shall define the phase separated fraction as the fraction of PVME units in concentrated, polymer-rich phase. We have determined the values of the fraction of phase-separated PVME units from the following relation

$$p\,(T) = 1 - \frac{I}{I_0} \tag{1}$$

where I is the integrated intensity of the given polymer line in a partly phase-separated system and I_0 is the integrated intensity of this line if no phase separation occurs [11,23].

Temperature dependences of the fraction p as obtained from integrated intensities of $CHOCH_3$ protons of PVME are shown for neat PVME solution (c_P = 5 wt %) and PVME solutions with c_{ad} = 5 wt % in Figure 3. For all polymer and additive concentrations investigated, the solutions show a qualitatively similar behavior of the polymer $CHOCH_3$ proton intensities. From Figure 3 it follows that all solutions with additives exhibit broader transition region than the solution with neat PVME; this effect is the most significant in PVME/TBMK solution where the transition is ~12 K broad. Transition temperature was detected as the temperature in the middle of the transition, *i.e.*, where the signal has decreased by 50%. Figure 4 shows the dependence of transition temperature on additive concentration for solutions with c_P = 5 wt %. For TBAm and TBOH, increasing concentration was observed to lead to a slight shift of transition temperature to higher values; at the same time the transition extent (fraction p above the transition in Figure 3) decreases as compared with the neat PVME. TBAm and TBOH molecules obviously stabilize polymer-solvent interactions and prevent hydrophobic polymer-polymer interactions. Such stabilizing effect was detected in aqueous solutions of PVME and lower molecular weight alcohols [15,18,22].

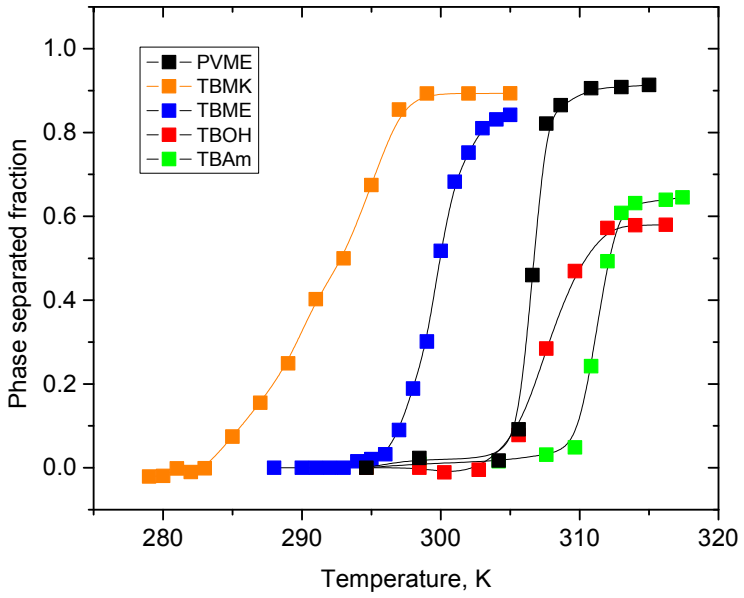

Figure 3. Temperature dependences of the fraction p as obtained from integrated intensities of $CHOCH_3$ protons of PVME in neat PVME solution (c_P = 5 wt % in D_2O) and PVME/additives solutions (c_P = 5 wt %, c_{ad} = 5 wt % in D_2O).

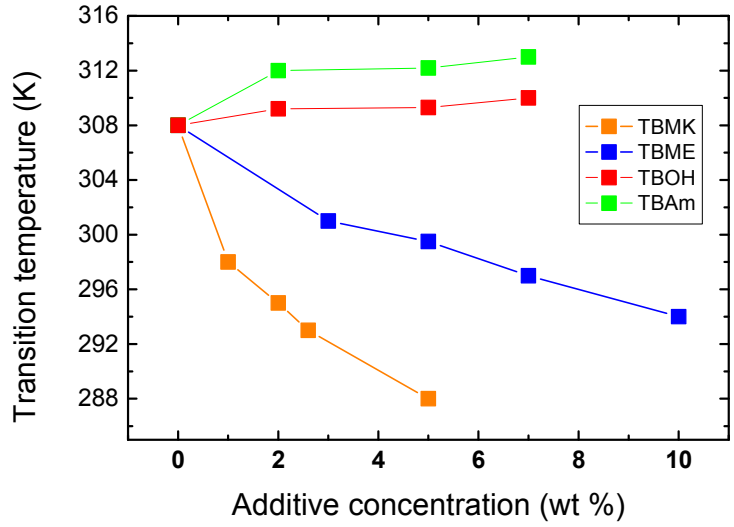

Figure 4. Concentration dependence of the transition temperature for PVME/additives solutions (c_P = 5 wt % PVME in D_2O).

On the other hand, increasing the concentration of the additives TBMK and TBME in the system promotes destabilization of the hydration structure surrounding the polymer chain; increasing this concentration significantly decreases the transition temperature. As shown in Figure 4, this effect is more pronounced for TBMK. The presence of the ether additive only results in changes of the transition temperature, and no broadening of the transition region was observed. Similarly as TBMK and TBME, higher alcohols, and simple inorganic salts tend to destabilize the structure, *i.e.*, lead to lower transition temperatures in aqueous solutions of PVME [18]. The values of fraction p above the transition in PVME/TBMK and PVME/TBME solutions reach ~0.9 similarly as the values in neat PVME solution. We assume that the remaining minority mobile component (~10%), which does not take part in the phase transition, comes from low-molecular weight oligomers as it was shown for PVME/D_2O solutions [24].

The effect of polymer concentration on the phase transition of solutions with hydrophilic and hydrophobic additives (TBAm and TBME, respectively) is seen in Figure 5. For higher PVME concentrations (c_p = 10 wt %) in PVME/TBAm solution, the dependence is shifted by ~4 K to lower values. This shift of the transition is probably a consequence of the preferred polymer-polymer contacts at higher concentration, allowing hydrophobic interactions to predominate at lower temperatures. More complicated behavior was detected for solutions with hydrophobic TBME. An increase of the transition temperature is observed for additive concentration c_{ad} = 3 wt % and higher polymer concentration, apparently since the number of hydrophobic additive molecules per polymer segment decreases and, thus, hydrophobic interactions of the additive with the chain are reduced. Subsequently, for more concentrated polymer solutions and c_{ad} > 5 wt %, the transition temperature decreases by ~4 K. The solvent quality for such high TBME concentrations is probably reduced and the phase transition occurs already at lower temperatures. These two different mechanisms controlling LCST shift were described for aqueous solutions of poly(*N*-isopropylacrylamide) and hydrophobic benzaldehydes [19].

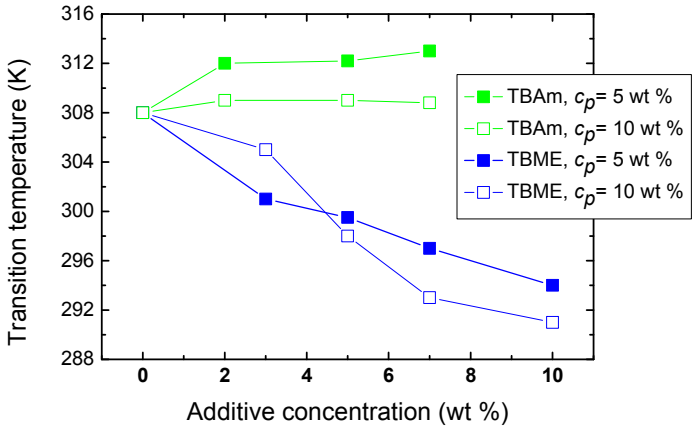

Figure 5. Concentration dependence of the transition temperature for PVME/TBME and PVME/TBAm solutions for two various polymer concentrations c_P = 5 and 10 wt % PVME in D_2O.

3.2. Mobility of Water and Additive Molecules during Phase Transition

The mobilities of the additive and water molecules were studied using NMR spin-spin relaxation time T_2 [5,11]. To follow the changes in the behavior of the water and additive in the presence of the polymer, a comparative analysis of T_2 was performed at temperatures below and above the transition. In this respect it is useful to define T_{2im} as the ratio of the measured T_2 values in the polymer-additive system $T_{2(pvme+additive)}$ and in the corresponding additive/D_2O solution $T_{2(additive)}$ at the same temperature (T_{2im} = $T_{2(pvme+additive)}/T_{2(additive)}$) [20]. The value of T_{2im} gives temperature-independent information about the extent of the immobilization of the water and additive molecules caused by the presence of the polymer. The comparison of these quantities for HDO molecules and for the *t*-butyl group of the additives is given in Table 1. If no interaction with the polymer occurs, the value of T_{2im} should be equal to 1 (if the effects of viscosity can be neglected). The lower the resulting value, the higher the immobilization effect caused by the polymer–water or polymer–additive interaction.

Table 1. T_{2im} parameters for the PVME/additive solutions (c_P = 5 wt %, c_{ad} = 5 wt %).

Temperature	TBMK		TBME		TBOH		TBAm	
	HDO	$(CH_3)_3$	HDO	$(CH_3)_3$	HDO	$(CH_3)_3$	HDO	$(CH_3)_3$
below LCST	0.16	0.42	0.78	0.78	0.65	0.92	0.60	0.88
above LCST	0.14	0.32	0.60	0.54	0.34	0.30	0.83	0.79

Relaxation parameters T_{2im} detected in PVME/TBOH and PVME/TBAm solutions below LCST reach similar values, see Table 1. T_{2im} values of the additive *t*-butyl group are almost equal to 1, values as obtained for water molecules are somewhat lower which could indicate a slight interaction with the polymer as well as the influence of chemical exchange. Different relaxation behavior of molecules in solutions with hydrophilic additives was found at elevated temperatures above LCST. T_{2im} values of molecules in PVME/TBAm solution remain high even above the transition while a reduction of T_{2im} values was observed for water and additive molecules in PVME/TBOH solution. The greater immobilization above the transition temperature for TBOH and water can be attributed to the effect of incorporation of a certain portion of these molecules into the globular structures.

Changes in the mobility of solvent molecules as a function of time were found to arise from the effects of solvent molecules being released from the polymer globular structure. The investigated samples were kept for the whole time in the magnet of NMR spectrometer at elevated temperature and the time dependence of T_2 values was measured. Figure 6a shows that T_2 values of HDO and *t*-butyl group in the PVME/TBOH solution very slowly increased with time, reaching after tens of hours a value similar to that observed at temperatures below the transition. These results provide evidence that water and additive originally bound in globules are, over time, very slowly released (squeezed out) from the globular structures. Such behavior was previously detected in aqueous solutions of neat PVME solutions [5,11]. In contrast, for TBAm solutions no such changes in T_2 as a function of time were observed, confirming the idea that globules formed in these solutions do not contain bound water or/and additive.

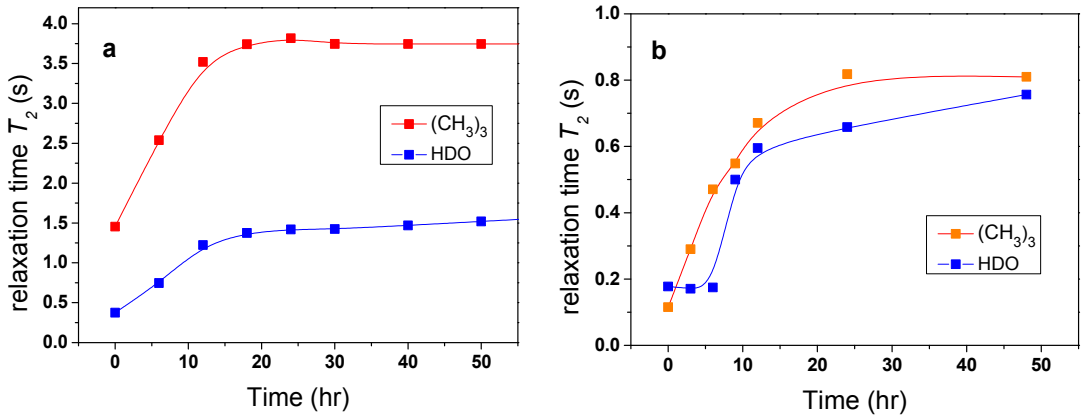

Figure 6. Time dependences of the spin-spin relaxation time T_2 of HDO and $(CH_3)_3$ protons of additive in PVME/TBOH (**a**) and PVME/TBMK (**b**) solutions (c_P = 5 wt %, c_{ad} = 5 wt % in D_2O) measured above the phase transition.

It follows from Table 1 that, for the solution with TBMK, T_{2im} of water and *t*-butyl group reach substantially lower values indicating that water and additive molecules are strongly involved in interactions with the polymer at temperatures both below and above LCST. For TBME, the solvent and additive molecules are only slightly affected by the presence of the polymer. Similarly as in the case of PVME/TBOH solutions, a time-dependent experiment (Figure 6b) confirmed that molecules originally bound in collapsed polymer structures of PVME/TBMK solution are slowly released.

3.3. FTIR Spectroscopy

As indicated by the concentration dependences of the transition temperature in Figure 4 and NMR relaxations, solutions with TBMK and TBME showed substantial differences during phase transition. A detailed FTIR study confirmed different interaction mechanisms taking place in these solutions. On the other hand, no or negligible differences were recorded in FTIR spectra of PVME/TBOH and PVME/TBAm solutions and they were, thus, no longer analyzed.

Corrected ATR FTIR spectra of TMBK systems are presented in Figure 7. In the presence of two PVME bands that are assigned to the stretching vibration of the carbonyl group of TBMK are present at 278 K (spectrum d in Figure 7); one band is at 1705 cm^{-1}, which is close to the position of the band for the neat form of the compound (spectrum a) [25], and a second band is at 1688 cm^{-1}, which corresponds to the hydrated form of TBMK (spectra b and c). As the temperature increases to 301 K (well above LCST), only the band that represents the neat form is present at 1707 cm^{-1}. In the presence of PVME, the positions the symmetric CH_3 deformation bands are almost identical to the locations of the bands in the neat TBMK (1365 cm^{-1} and 1355 cm^{-1}). The above observations could signify that below the transition temperature, domains rich in TBMK and attached to the polymer exist. The surfaces of these domains interact with water molecules through hydrogen bonds with the carbonyl groups of TBMK; thus, two carbonyl bands are present in the spectra below the transition—a hydrated band and a band similar to the neat TBMK. Above the transition temperature, the methyl groups remain in the same environment, whereas the carbonyl groups experience an environment similar to that of the neat TBMK and are no longer in contact with water molecules—this result could be consistent with the entrance of TBMK into the interior of the collapsed PVME globules.

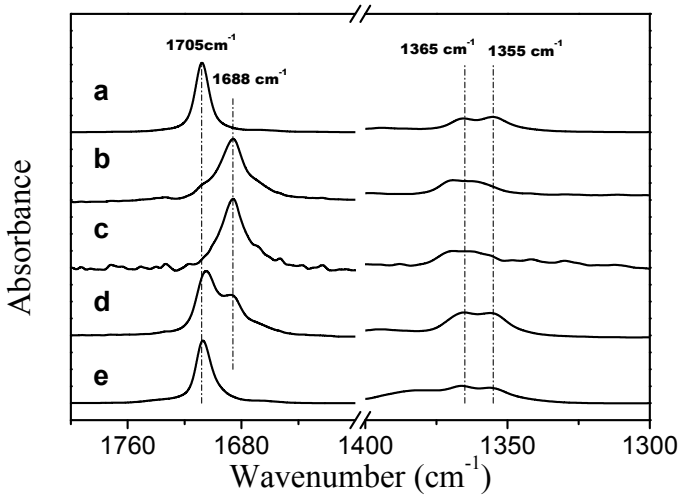

Figure 7. Corrected ATR FTIR spectra of TMBK at a temperature of 301 K (**a**); TBMK in D_2O at a concentration of 5 wt % and a temperature 278 K (**b**); TBMK in D_2O at a concentration of 5 wt % and a temperature 301 K (**c**); PVME/TBMK/D_2O at c_P = 0.5 wt % and c_{ad} = 5 wt % and a temperature of 278 K (**d**); and PVME/TBMK/D_2O at c_P = 0.5 wt % and c_{ad} = 5 wt % and a temperature of 301 K (**e**).

In the spectrum of neat TBME, the CH_3 symmetric deformation bands are located at 1386 and 1364 cm^{-1} (spectrum Figure 8a). In the presence of PVME the positions of these two bands are identical to the locations of the bands in the spectra of TBME hydrated with D_2O at 278 K. Upon an increase in temperature to 301 K (above LCST), these two bands shift to positions identical to those in neat TBME. In the spectrum of neat TBME, the band assigned to the C–O stretching vibration of the methoxy group is located at 1086 cm^{-1} [26]. An appearance of the second band at 1046 cm^{-1}, in the presence of PVME, most likely corresponds to the hydrated form of TBME. The above observations confirm that below the transition temperature the methyl groups of TBME are hydrated. Above the transition temperature, the methyl groups are located in an environment similar to neat TBME. The two C–O stretching vibration bands in the methoxy group that are present in the spectra below and above the transition temperature (spectra Figure 8d,e) indicate the presence of two types of additive molecules; the α band most likely corresponds to TBME molecules that are isolated from each other and in which the dipole-dipole intermolecular interaction has been eliminated. The β band at the lower wavenumbers probably corresponds to hydrated TBME molecules in which the methoxy oxygen is involved in hydrogen bonds with the solvating D_2O molecules.

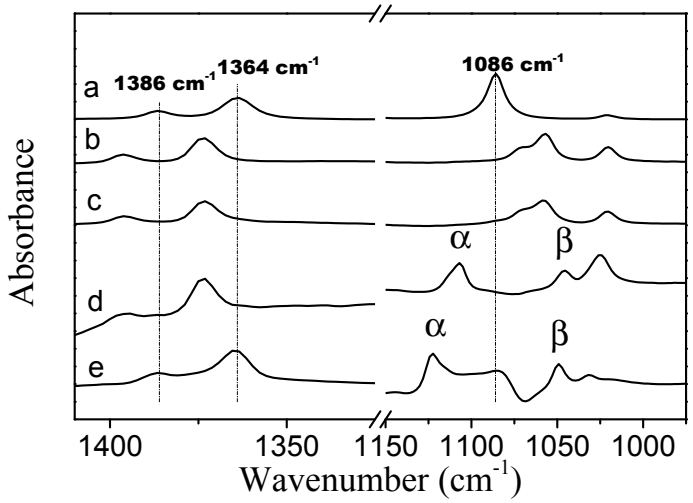

Figure 8. Corrected ATR FTIR spectra of (**a**) TBME at a temperature of 301 K; (**b**) TBME in D_2O at a concentration of 5 wt % and a temperature of 278 K; (**c**) TBME in D_2O at a concentration of 5 wt % and a temperature of 301 K; (**d**) PVME/TBME/D_2O at c_P = 10 wt % and c_{ad} = 5 wt % and a temperature of 278 K; and (**e**) PVME/TBME/D_2O at c_P = 10 wt % and c_{ad} = 5 wt % and a temperature of 301 K.

From the results obtained from NMR relaxation and FTIR experiments, we can suggest that globular structures formed in TBME solutions above LCST do not contain a substantial amount of bound water or additive molecules; the slight mobility restriction of water and TBME could be caused by interactions of these molecules with the surface of the polymer globules. On the other hand, for TBMK solutions we observe a strong mobility reduction of the additive and water molecules. This fact can be explained by the interactions between the polymer chain and the TBMK carbonyl group that are mediated by one or more water molecules.

3.4. Cooperativity of the Phase Transition

The temperature dependences of *p*-fraction shown in Figure 3 can be used for determining the enthalpy and entropy changes during phase transition, considering this process as the competition between non-phase separated (coil) and phase separated (globule) states governed by the Gibbs free energy. The van´t Hoff equation describes temperature changes of the equilibrium constant *K* of the coil-globule transition as follows:

$$\ln K = -\frac{\Delta H_{NMR}}{RT} + \frac{\Delta S_{NMR}}{T} \quad (2)$$

where ΔH_{NMR} and ΔS_{NMR} are the changes in enthalpy and entropy, respectively, and *R* is the gas constant. In relation to the *p*-fraction the equilibrium constant *K* can be written as the ratio:

$$K = \frac{p}{p_{max} - p} \quad (3)$$

where p_{max} are values of fraction *p* above the transition. The dependences of $R \ln(p/(p_{max} - p))$ on $-1/T$ were fitted with linear regression according to Equations (2) and (3) and the parameters ΔH_{NMR} are summarized in Table 2. Table 2 contains also enthalpy changes ΔH_{DSC} as obtained from DSC measurements and recalculated to mol of monomer units where the enthalpy data for neat PVME quite well agree with the literature [27,28]. Enthalpy values ΔH_{DSC} can be compared with those determined from NMR. Assuming that the phase transition is a cooperative process and the polymer chain consists of cooperative units (domains) which undergo transition as a whole [29–31], the values ΔH_{NMR} are thus related to mol of cooperative units. The ratio $\Delta H_{NMR}/\Delta H_{DSC}$ represents the average number

of monomer units in one cooperative domain and can provide a quantitative analysis of the degree of cooperativity (*cf.* Table 2). For the 5 wt % solution of neat PVME and solutions of PVME with TBME and TBAm (c_{ad} = 5 wt %), the size of the domains agrees quite well with the average degree of polymerization (D_P of PVME ~348), thus showing that, in this case, the cooperative unit is the whole polymer chain. For solutions with TBMK and TBOH (c_{ad} = 5 wt %), these domains are smaller and consist of only 140 and 170 monomer units, respectively. As follows from relaxation experiments, a certain amount of water and additive molecules is incorporated into the globules formed in these two solutions. This process is obviously time-consuming and disrupts the cooperativity of the transition; cooperative units are smaller and the phase transition is broader.

Table 2. Thermodynamic parameters determined by NMR and DSC and the number of monomer units in the domain for mixtures of 5 wt % PVME.

Sample	ΔH_{NMR} MJ/mol	ΔH_{DSC} kJ/mol	Number of Mon. Units in Domain
PVME	1.32	4.05	326
TBMK	0.32	2.23	143
TBME	0.78	2.32	336
TBOH	0.40	2.30	174
TBAm	0.58	1.98	293

The difference in the structure and size of the polymer globules in the presence of the additives can be demonstrated by the optical microscopy images shown in Figure 9. This figure demonstrates that globular structures formed above LCST transition in aqueous PVME/TBMK and PVME/TBOH solutions are somewhat smaller than those observed for solutions with other additives and neat PVME. This finding corresponds to the data in Table 2 where size of cooperative domains as calculated for PVME/TBOH and PVME/TBMK solutions is about twice smaller in comparison with domains formed in other solutions and this is obviously macroscopically manifested in smaller polymer aggregations. Interestingly enough, polymer agglomerates formed in PVME/TBME solutions show strong separation and well-defined surfaces. This could be the consequence of the fact that 90% of polymer chains are involved in the collapsed structures, as follows from the fraction p above the transition, and at the same time these structures do not contain any bound water or additive.

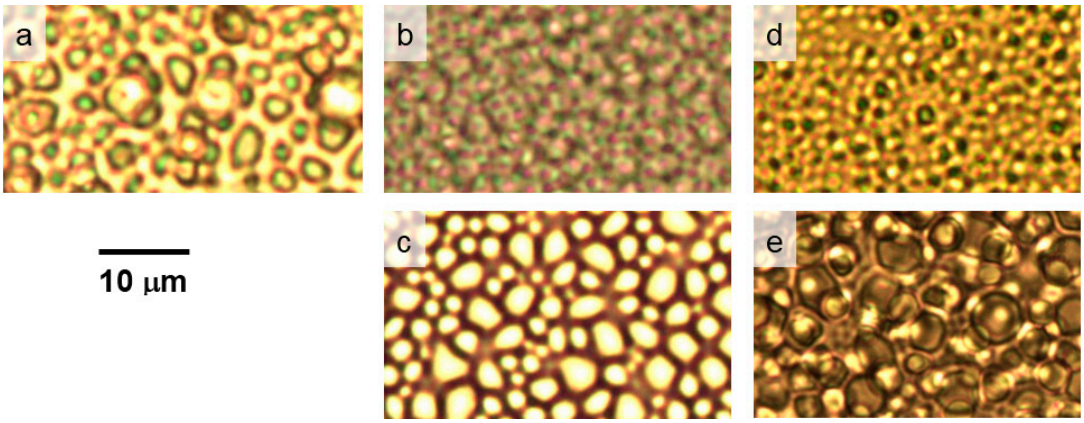

Figure 9. Photomicrographs of the neat PVME solution (c_P = 5 wt % in D_2O) (**a**) and solutions with additives TBMK (**b**); TBME (**c**); TBOH (**d**); and TBAm (**e**) (c_P = 5 wt %, c_{ad} = 5 wt %) recorded at temperatures above the transitions of the particular systems.

4. Conclusions

Temperature-induced phase separation of PVME in the presence of small additives was investigated with various techniques. It has been shown that the interactions and dynamics during the phase transition are significantly influenced by the chemical structure of an additive molecule and hydrophobic additives more strongly affect polymer transition than additives with hydrophilic character. A slight stabilizing effect of hydrogen bonding was manifested in the presence of hydrophilic additives TBOH and TBAm in PVME solution by the shift of the transition region towards higher temperatures and by a decrease of the fraction of PVME units involved in globular structures. A clear pronounced decreasing effect on the LCST was found for hydrophobic TBME and TBMK additives, which obviously facilitate the phase separation process. Detailed FTIR analysis showed that TBMK is in a strong interaction with the carbonyl group of the additive and the ether group of the polymer even before phase transition, in contrast to TBME, with which no polymer interaction occurs before the transition. Two different mechanisms controlling LCST shift were suggested from polymer concentration dependences.

From comparison of thermodynamical parameters, as obtained from NMR and DSC, the size of the cooperative units undergoing the transition as a whole was determined. Cooperative domains in PVME/TBOH and PVME/TBMK solutions are about twice smaller in comparison with those formed in other solutions, and this is macroscopically manifested in smaller polymer aggregations. NMR relaxation experiments confirmed that a certain portion of water and additive molecules remained bound in PVME globules in the solutions with TBOH and TBMK. The incorporation of water and additive molecules into the globules, thus, leads to reduced cooperativity of the transition and influences the size of polymer aggregations formed above LCST. The originally-bound molecules are, over time, very slowly released from phase-separated globules.

Acknowledgments: Support by the Czech Science Foundation (Project 13-23392S) is gratefully acknowledged.

Author Contributions: Larisa Starovoytova, Nadiia Velychkivska and Rafal Konefal performed NMR experiments and analyzed NMR data; Julie Šťastná performed experiments on optical microscopy; Adriana Šturcová and Jiří Dybal performed FTIR experiments and analyzed FTIR data; Marek Radecki performed experiments on optical microscopy and DSC; Lenka Hanyková and Larisa Starovoytova wrote the paper.

Conflicts of Interest: The authors declare no conflict of interest.

References

1. Liu, R.; Fraylich, M.; Saunders, B.R. Thermoresponsive copolymers: From fundamental studies to applications. *Colloid Polym. Sci.* **2009**, *287*, 627–643. [CrossRef]
2. Aseyev, V.O.; Tenhu, H.; Winnik, F.M. Temperature dependence of the colloidal stability of neutral amphiphilic polymers in water. *Adv. Polym. Sci.* **2006**, *196*, 1–85.
3. Schild, H.G. Poly(*N*-isopropylacrylamide)—Experiment, theory and application. *Prog. Polym. Sci.* **1992**, *17*, 163–249. [CrossRef]
4. Aseyev, V.O.; Tenhu, H.; Winnik, F.M. Non-ionic thermoresponsive polymers in water. *Adv. Polym. Sci.* **2011**, *242*, 29–89.
5. Spěváček, J.; Hanyková, L.; Starovoytova, L. ^{1}H NMR relaxation study of thermotropic phase transition in poly(vinyl methyl ether)/D_2O solutions. *Macromolecules* **2004**, *37*, 7710–7718. [CrossRef]
6. Zeng, X.; Yang, X. A study of interaction of water and model compound of poly(vinyl methyl ether). *J. Phys. Chem. B* **2004**, *108*, 17384–17392. [CrossRef]
7. Pastorczak, M.; Kozanecki, M.; Ulanski, J. Water-polymer interactions in PVME hydrogels—Raman spectroscopy studies. *Polymer* **2009**, *50*, 4535–4542. [CrossRef]
8. Van Durme, K.; Loozen, E.; Nies, E.; Mele, B. Phase behavior of poly(vinyl methyl ether) in deuterium oxide. *Macromolecules* **2005**, *38*, 10234–10243. [CrossRef]
9. Meeussen, F.; Bauwens, Y.; Moerkerke, R.; Nies, E.; Berghmans, H. Molecular complex formation in the system poly(vinyl methyl ether)/water. *Polymer* **2000**, *41*, 3737–3743. [CrossRef]

10. Maeda, H. Dielectric and calorimetric behaviors of poly(viny1 methyl ether)–water systems including unusual relaxation processes at subzero temperatures. *Macromolecules* **1995**, *28*, 5156–5159. [CrossRef]
11. Starovoytova, L.; Spěváček, J. Effect of time on the hydration and temperature-induced phase separation in aqueous polymer solutions. ^{1}H NMR study. *Polymer* **2006**, *47*, 7329–7334. [CrossRef]
12. Hanyková, L.; Spěváček, J.; Ilavský, M. ^{1}H NMR study of thermotropic phase transition of linear and crosslinked poly(vinyl methyl ether) in D_2O. *Polymer* **2001**, *42*, 8607–8612. [CrossRef]
13. Sun, B.; Lai, H.; Wu, P. Integrated microdynamics mechanism of the thermal-induced phase separation behavior of poly(vinyl methyl ether) aqueous solution. *J. Phys. Chem. B* **2011**, *115*, 1335–1346. [CrossRef] [PubMed]
14. Maeda, Y. IR spectroscopic study on the hydration and the phase transition of poly(vinyl methyl ether) in water. *Langmuir* **2001**, *17*, 1737–1742. [CrossRef]
15. Labuta, J.; Hill, J.P.; Hanyková, L.; Ishihara, S.; Ariga, K. Probing the micro-phase separation of thermo-responsive amphiphilic polymer in water/ethanol solution. *J. Nanosci. Nanotech.* **2010**, *10*, 8408–8416. [CrossRef]
16. Van Durme, K.; Rahier, H.; Mele, B. Influence of additives on the thermoresponsive behavior of polymers in aqueous solution. *Macromolecules* **2005**, *38*, 10155–10163. [CrossRef]
17. Housni, A.; Narain, R. Aqueous solution behavior of poly(*N*-isopropylacrylamide) in the presence of water-soluble macromolecular species. *Eur. Polym. J.* **2007**, *43*, 4344–4354. [CrossRef]
18. Horne, R.A.; Almeida, J.P.; Day, A.F.; Yu, N.T. Macromolecule hydration and the effect of solutes on the cloud point of aqueous solutions of polyvinyl methyl ether: A possible model for protein denaturation and temperature control in homeothermic animals. *J. Colloid Interface Sci.* **1971**, *35*, 78–84. [CrossRef]
19. Hofmann, C.; Schonhoff, M. Do additives shift the LCST of poly(*N*-isopropyl acrylamide) by solvent quality changes or by direct interactions? *Colloid Polym. Sci.* **2009**, *287*, 1369–1376. [CrossRef]
20. Hofmann, C.; Schonhoff, M. Dynamics and distribution of aromatic model drugs in the phase transition of thermoreversible poly(*N*-isopropyl acrylamide) in solution. *Colloid Polym. Sci.* **2012**, *290*, 689–698. [CrossRef]
21. Costa, R.; Freitas, R. Phase behavior of poly(*N*-isopropyl acrylamide) in binary aqueous solutions. *Polymer* **2002**, *43*, 5879–5885. [CrossRef]
22. Maeda, Y.; Yamamoto, H.; Ikeda, I. Micro-Raman spectroscopic investigation on the phase separation of poly(vinyl methyl ether)/alcohol/water ternary mixtures. *Langmuir* **2004**, *20*, 7339–7341. [CrossRef] [PubMed]
23. Spěváček, J.; Hanyková, L. NMR study on polymer-solvent interactions during temperature-induced phase separation in aqueous polymer solutions. *Macromol. Symp.* **2007**, *251*, 72–80. [CrossRef]
24. Spěváček, J.; Hanyková, L. ^{1}H NMR relaxation study of polymer-solvent interactions during thermotropic phase transition in aqueous solutions. *Macromol. Symp.* **2003**, *203*, 229–238. [CrossRef]
25. Crowder, G.A. 3,3-Dimethyl-2-butanone: Infrared and Raman spectra, normal coordinate calculations, and calculated structure. *Spectrosc. Lett.* **1997**, *30*, 1353–1367. [CrossRef]
26. Li, Z.; Singh, S. FTIR and ab-initio investigations of the MTBE—Water complex. *J. Phys. Chem. A* **2008**, *112*, 8593–8599. [CrossRef] [PubMed]
27. Maeda, H.J. Interaction of water with poly(vinyl methyl ether). *J. Polym. Sci.* **1994**, *32*, 91–97. [CrossRef]
28. Schafer-Soenen, H.; Moerkerke, R.; Berghmans, H.; Koningsveld, R.; Dušek, K.; Šolc, K. Zero and off-zero critical concentrations in systems containing polydisperse polymers with very high molar masses. 2. The system water—Poly(vinyl methyl ether). *Macromolecules* **1997**, *30*, 410–416. [CrossRef]
29. Tiktopulo, E.I.; Uversky, V.N.; Lushchik, V.B.; Klenin, S.I.; Bychkova, V.E.; Ptitsyn, O.B. "Domain" coil-globule transition in homopolymers. *Macromolecules* **1995**, *28*, 7519–7524. [CrossRef]
30. Tiktopulo, E.I.; Bychkova, V.E.; Ricka, J.; Ptitsyn, O.B. Cooperativity of the coil-globule transition in a homopolymer: Microcalorimetric study of poly(*N*-isopropylacrylamide). *Macromolecules* **1994**, *27*, 2879–2882. [CrossRef]
31. Hanyková, L.; Radecki, M. NMR and thermodynamic study of phase transition in aqueous solutions of thermoresponsive amphiphilic polymer. *Chem. Lett.* **2012**, *41*, 1044–1046. [CrossRef]

Publication № 2

Colloid Polym Sci
DOI 10.1007/s00396-017-4100-2

INVITED ARTICLE

Thermodynamic and kinetic analysis of phase separation of temperature-sensitive poly(vinyl methyl ether) in the presence of hydrophobic *tert*-butyl alcohol

Nadiia Velychkivska[1] · Anna Bogomolova[1] · Sergey K. Filippov[1] · Larisa Starovoytova[1] · Jan Labuta[2]

Received: 28 January 2017 / Revised: 17 April 2017 / Accepted: 17 April 2017

Abstract NMR and isothermal titration calorimetry (ITC) techniques were chosen to examine interactions in a poly(vinyl methyl ether) (PVME)/*tert*-butyl alcohol (*t*-BuOH)/water ternary system. The effects of PVME and *t*-BuOH concentrations on phase separation temperature were examined. Molecules of *t*-BuOH additive hydrophobically associate with PVME and decrease the phase separation temperature. Thermodynamic parameters connected with phase separation were calculated from NMR results using an approach based on the van't Hoff equation. Presence of *t*-BuOH increases the number of PVME monomeric units in one cooperative domain (where the units undergo phase separation as whole—'all-or-none'). NMR time-resolved relaxation measurements show very different dynamics of the solvent releasing process for low and high PVME concentrations above phase separation temperature. ITC data show that the presence of *t*-BuOH restricts water solvation of PVME globules. Presented results on the PVME/*t*-BuOH/D_2O system show that the PVME solution properties are *not* constant in time. The analysis of measurements (and resulting properties) should always be done while considering strong time-dependent behaviour of PVME solutions.

Keywords Phase separation · Coil–globule transition · Poly(vinyl methyl ether) · *tert*-Butyl alcohol · Nuclear magnetic resonance · Isothermal titration calorimetry

✉ Jan Labuta
Labuta.Jan@nims.go.jp

[1] Institute of Macromolecular Chemistry, AS CR, Heyrovsky Sq. 2, 162 06 Prague, Czech Republic

[2] International Center for Materials Nanoarchitectonics (WPI-MANA), National Institute for Materials Science (NIMS), 1-1 Namiki, Tsukuba, Ibaraki 305-0044, Japan

Introduction

Stimuli-responsive polymers are a class of materials capable of changing their solution behaviours under the influence of temperature, light or other external stimuli [1–7]. The change in solution behaviour is usually referred to as the coil-to-globule transition, when initially completely soluble polymer chain (coil) phase separate to dense globules. In the cases when a transition takes place with a temperature increase, the polymer is called temperature-sensitive with a characteristic value of lower critical solution temperature (LCST). This phenomenon is often observed in polymers with amphiphilic character, such as acrylamide-based polymers [8–10]. Another typical example is poly(vinyl methyl ether) (PVME) with LCST around 308 K (35 °C). The proximity of an LCST to normal human body temperatures makes this polymer interesting for various medical applications [11]. Interestingly, PVME has a type III LCST phase diagram with two critical points (minima). This is rationalized within the framework of Flory-Huggins theory by a concentration dependence of the interaction parameter χ [12, 13]. The phase separation mechanism of PVME has been extensively investigated by a number of different methods such as nuclear magnetic resonance (NMR) [14–22], infrared spectroscopy [20, 21, 23–25], Rayleigh scattering [26], differential scanning calorimetry [12, 13, 17, 20, 25, 27], optical microscopy [17, 20], Raman spectroscopy [28] and ab initio calculations [24].

The interactions of stimuli-responsive polymers with low molecular weight compounds are still of interest since an addition of small molecules, such as surfactant, salt or alcohol, can affect the phase separation properties. Additive molecules are sometimes used as a model system for drug delivery applications [29]. It was shown that the addition of small molecules (additive) to aqueous polymer solution can shift the phase separation temperature (T_p) and the amount of polymer

Published online: 11 May 2017

groups participating in phase separation. The effects of surfactants, ions and salts, on the phase separation phenomenon, are well documented [9, 20, 30–33]. Micro-Raman spectroscopic study [34] of PVME with several alcohols (methanol, ethanol, 2-propanol and *t*-butanol) shows that higher (relatively more hydrophobic) alcohols associate with PVME more easily which increases the overall hydrophobicity of PVME/alcohol complexes and thus reducing T_p. Relatively less hydrophobic alcohols (such as ethanol) [16] exhibit the opposite behaviour and increase T_p. The studies are often concentrated on the determination of T_p as a function of additive type and concentration. This approach does not always provide a deeper insight into specific interactions between a polymer and an additive. In order to probe these interactions on a molecular level [19, 35, 36], we employed NMR spectroscopy and isothermal titration calorimetry (ITC) techniques.

In this work, we characterize the effects of a relatively (compared to methanol) hydrophobic *tert*-butyl alcohol (*t*-BuOH) additive on the phase separation of PVME paying particular attention to the behaviour of *t*-BuOH and water molecules below and above T_p. The temperature-dependent phase-separated fraction of PVME as a function of the additive and polymer concentrations is investigated by means of ^{1}H NMR spectroscopy. The obtained results are then modelled using a physicochemical model based on the van't Hoff equation to yield the thermodynamic parameters. The molecular mobility of *t*-BuOH and D_2O solvent molecules is studied using ^{1}H NMR spin–spin relaxation experiments (spin–spin relaxation time T_2). The dynamics of the releasing process of *t*-BuOH and D_2O from globular structures of PVME above T_p is investigated by using the time evolution of molecular mobility (T_2). The ITC technique, as a complementary method, probes the thermodynamics of *t*-BuOH interaction with PVME above and below T_p. ^{1}H NMR spin–spin relaxation experiments and ITC measurements complementarily describe the dynamics of the *t*-BuOH and D_2O interactions with PVME.

Materials and methods

PVME (purchased from Aldrich, supplied as 50 wt% aqueous solution; molecular weight determined by SEC in THF: M_w = 60,500 g/mol and $M_w/M_n \approx 3$ [15]; degree of polymerization ≈ 348; tacticity by ^{1}H NMR 59% of isotactic diads [22]) was used after drying to prepare PVME/D_2O solutions. The D_2O (Sigma, 99.9% of deuterium) solvent was used for the sample preparation. *tert*-Butyl alcohol (*t*-BuOH) (anhydrous, ≥99.5%, Sigma-Aldrich) was used as an additive to the polymer solutions. All samples were sealed in 5-mm NMR tubes. The weight fraction of PVME in binary solvent D_2O/*t*-BuOH is denoted as $c_P = m_P/(m_P + m_{D2O} + m_{t\text{-}Bu}) \times 100$ (in wt%). The composition of the binary solvent D_2O/*t*-BuOH, determined by the weight fraction of *t*-BuOH in D_2O/*t*-BuOH, is denoted as $c_{t\text{-}Bu} = m_{t\text{-}Bu}/(m_{D2O} + m_{t\text{-}Bu}) \times 100$ (in wt%), where m_x is the mass of each component.

High-resolution ^{1}H NMR spectra were recorded using a Bruker Avance III 600 spectrometer operating at 600.2 MHz. Measurement conditions were as follows: 90° pulse width 10 μs, relaxation delay 5 s, spectral width 9615 Hz, acquisition time 3.40 s and eight scans. The ^{1}H spin–spin relaxation times T_2 of *t*-BuOH and residual hydrogen-deuterium oxide (HDO) were measured at 600.2 MHz using a CPMG pulse sequence $90°_x - (t_d - 180°_y - t_d)_n -$ acquisition with half-echo time t_d = 5 ms. Every experiment was made using four scans with a relaxation delay between scans of 120 s. The obtained T_2 relaxation curves were mono-exponential. The fitting process made it possible to determine a single value of relaxation time. The relative error values of *t*-BuOH and HDO did not exceed ±5%. The temperature for all measurements was maintained at a constant within ±0.2 K in the range 295~325 K using a BVT 3000 temperature unit. The samples were kept at the experimental temperature for about 15 min prior to each measurement.

ITC measurements were performed on a MicroCal 200 isothermal titration calorimeter. The experiment was conducted with consecutive injections of *t*-BuOH solution into the calorimeter cell. The cell contained 280 μL of a polymer or water solution. The *t*-BuOH solution was added with a 40-μL injection syringe with a tip modified to act as a stirrer. The chosen stirring speed was 1000 rpm. The injection volume varied between 1 μL, for the first injection, and 2 μL, for the rest of the injections. The time between injections was 5 min. The measurements were conducted at 306, 308 and 310 K. The data were analysed using the Microcal ORIGIN software.

Results and discussion

An example of PVME phase separation (c_P = 5 wt%, $c_{t\text{-}Bu}$ = 2 wt%) as observed using variable temperature (VT) ^{1}H NMR is shown in Fig. 1. The spectra show clear beginning of phase separation around 308 K (≈35 °C) manifested by the appearance of broad resonance corresponding to phase-separated units of PVME (especially A and B groups) with a simultaneous decrease in intensity of non-separated PVME groups. At the same time, a slight broadening of the *t*-BuOH CH_3 group is observed, attributed to a fast chemical exchange between the *t*-BuOH complexed with PVME and free *t*-BuOH molecules. This suggests that the association of *t*-BuOH with PVME is rather weak.

Quantitative analyses of phase separation measurements shown in Fig. 1 are usually done via introducing

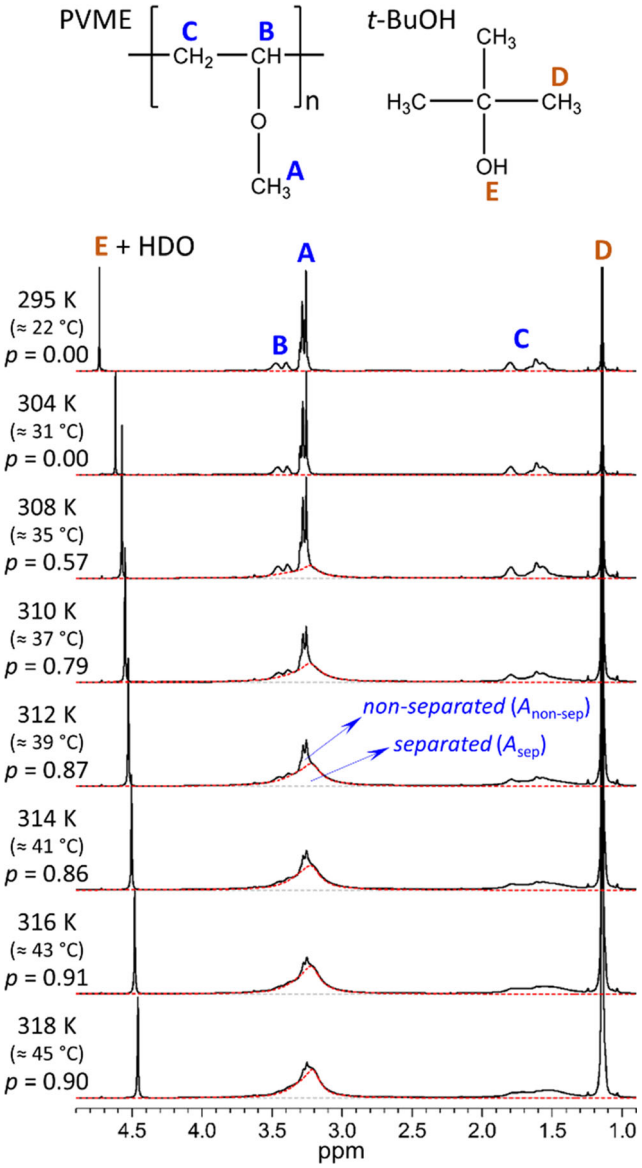

Fig. 1 VT-^{1}H NMR (600.2 MHz) of PVME (c_P = 5 wt%) in binary *t*-BuOH/D_2O solvent ($c_{t\text{-Bu}}$ = 2 wt%) measured from 295 to 318 K. Assignment of PVME and *t*-BuOH signals is shown in *top* spectrum. Key: *Black line* = spectrum, *red dashed line* = fit of broad separated part of PVME CH_3 and CH groups. Value of phase-separated fraction *p* is given for each spectrum

values of phase-separated fraction of PVME units $p(T)$ such as [19, 37] the following

$$p(T) = 1 - \frac{I'(T)}{I_0'(T_0)} = 1 - \frac{T}{T_0} \times \frac{I(T)}{I_0(T_0)} \quad (1)$$

where $I'(T)$ and $I_0'(T_0)$ are temperature-dependent integrated intensities of certain polymer resonance in a partly phase-separated system and before phase separation occurs, respectively. These values are unaffected by temperature dependence of integrated intensities. However, according to the Boltzmann equation during the measurement, we obtain extra decrease of integrated intensities with increasing absolute temperature as $1/T$. In order to correct this effect, values of integrated intensities as obtained from measurement $I(T)$ and $I_0(T_0)$ can be introduced using formulas $I(T) = I'(T)/T$ and $I_0(T_0) = I_0'(T_0)/T_0$, where $I(T)$ and $I_0(T_0)$ are Boltzmann uncorrected integrated intensities (as obtained from measurement) of partly phase-separated system and before phase separation occurs, respectively. This approach yields the right side of Eq. (1). As a result, Eq. (1) reflects only phase separation effects of the studied polymer system. $T \geq T_0$ is the temperature of actual measurement, and T_0 is the temperature at which no phase separation can be observed in the NMR spectrum. This approach contains several crude assumptions and is also dependent on the stability of the experimental setup during data collection. Therefore, we use a different method consisting of a spectral decomposition into phase-separated and non-separated parts by means of a careful fitting of each spectrum (see Fig. 1, dashed red lines). Up to two Lorentzian curves are used for fitting the broad phase-separated part of CH_3 and CH resonances of PVME (non-linear least square minimization method is adopted; linear function is taken as a baseline). This procedure gives the values of areas (integrated intensities) A_{sep} and $A_{non\text{-}sep}$ (see Fig. 1) corresponding to phase-separated and non-separated PVME units, respectively. The value of the phase-separated fraction $p(T)$ is simply defined as follows:

$$p(T) = \frac{A_{sep}}{A_{sep} + A_{non-sep}} \quad (2)$$

This method is independent of any assumption. It seems that the results of the *p* fraction, especially those well above phase separation temperature T_p, are more reliable. The *p* fraction data as obtained using this method for two PVME concentrations and several *t*-BuOH concentrations are shown in Fig. 2a, b. Additionally, the comparison of NMR spectra processing based on Eqs. 1 and 2 is shown in Fig. 2b, c (data in Fig. 2c are affected by systematic error which yields wider error bars).

A detail analysis of thermodynamic aspects of *p*, prior to the interpretation of *p*-fractions in Fig. 2, is given in the following text. We can assume that the phase separation process is a reversible chemical reaction between two states (non-separated and separated states) of PVME units. This reaction in equilibrium is described by equilibrium constant *K*, defined as a ratio of separated $N_{separated}$ and separable (but not separated yet) $N_{separable}$ PVME units (see Eq. 3). This model takes into consideration that some PVME units (e.g. low molecular

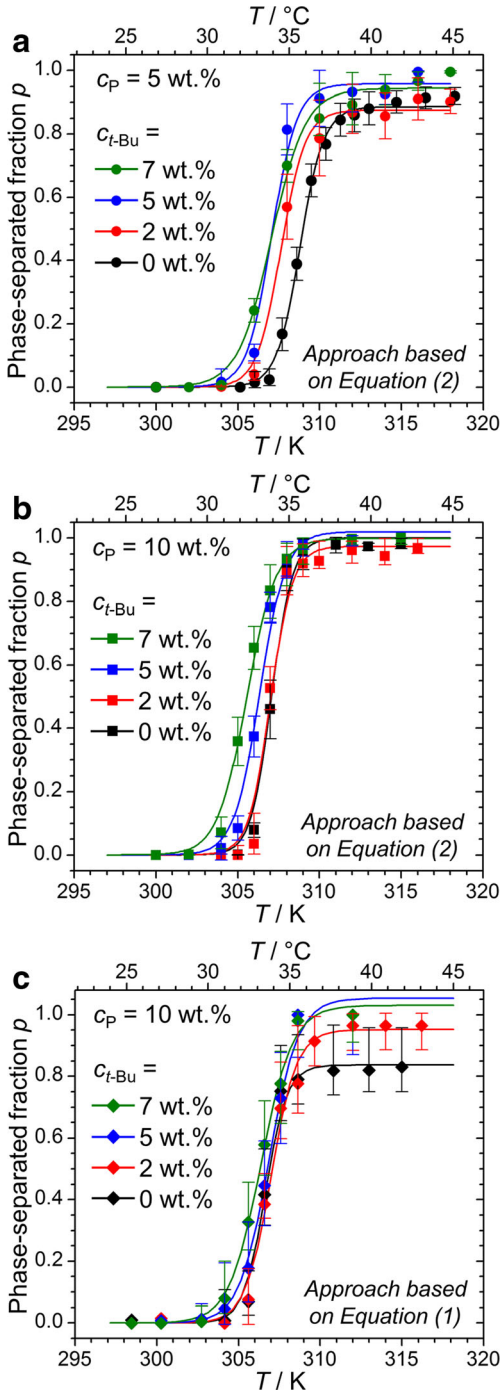

Fig. 2 Temperature dependences of phase-separated fraction p as obtained from CH_3 and CH resonances of PVME using fitting of VT-^{1}H NMR spectra (see Fig. 1). **a** 5 wt% and **b** 10 wt% of PVME (c_P) in binary mixture of D_2O/*t*-BuOH with four different *t*-BuOH concentrations ($c_{t\text{-Bu}}$) processed using approach based on Eq. 2. **c** Processing of the same samples as in **b** using approach based on Eq. 1 (higher estimated errors can be seen). Key: *full symbols* = experimental points; *error bars* correspond to confidence interval 2σ; *full lines* = fits according to Eq. 7

fractions) are inseparable (p does not reach 1 at high temperature) [15] which is expressed by $N_{\text{inseparable}}$ value. The model is schematically shown in Fig. 3.

$$K = \frac{N_{\text{separated}}}{N_{\text{separable}}} \tag{3}$$

In this framework, NMR experiments give value of the p-fraction as a ratio of separated $N_{\text{separated}}$ to all ($N_{\text{separable}}$ + $N_{\text{inseparable}}$ + $N_{\text{separated}}$) PVME units (see Eq. 4).

$$p(T) = \frac{N_{\text{separated}}}{N_{\text{separable}} + N_{\text{inseparable}} + N_{\text{separated}}} \tag{4}$$

Combination of Eqs. 3 and 4 yields a formula for p as a function of K:

$$p(T) = \frac{p_{\max}}{1 + K^{-1}} \tag{5}$$

where $p_{\max} = (N_{\text{separable}} + N_{\text{separated}})/(N_{\text{separable}} + N_{\text{inseparable}} + N_{\text{separated}})$ is the maximum fraction of PVME which can be phase separated. The connection between thermodynamic parameters and K is given by the van't Hoff equation:

$$K = e^{-\frac{\Delta H - T\Delta S}{RT}} \tag{6}$$

where ΔH and ΔS are the standard changes of enthalpy and entropy, respectively, connected with phase separation of PVME. R is the gas constant and T is the absolute temperature. Combination of Eqs. 5 and 6 gives the final form of p-fraction as a function of temperature with three well-defined and thermodynamically meaningful parameters:

$$p(T) = \frac{p_{\max}}{1 + e^{\frac{\Delta H}{RT} - \frac{\Delta S}{R}}} \tag{7}$$

NMR experimental data plotted in Fig. 2 are fitted using Eq. 7. The results are shown in Fig. 4. Five parameters were extracted from this fitting procedure: (1) phase separation temperature T_p (obtained as the onset temperature of the sigmoidal $p(T)$ curve constructed as an intersect point between tangent at inflexion point of $p(T)$ and x-axis), (2) maximum fraction of phase-separable PVME units $p_{\max}$, (3) width of phase separation ΔT_{width} (the difference between offset and onset temperatures),

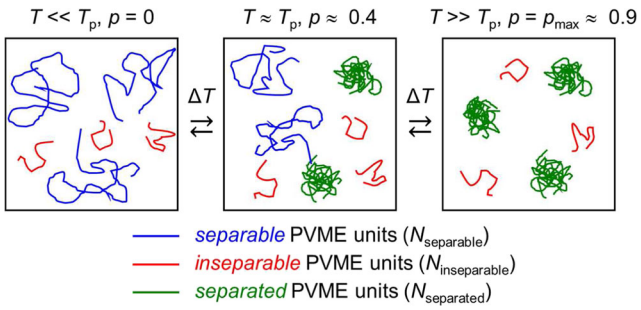

Fig. 3 Schematic description of phase separation model with three types of PVME units used for construction of thermodynamic model

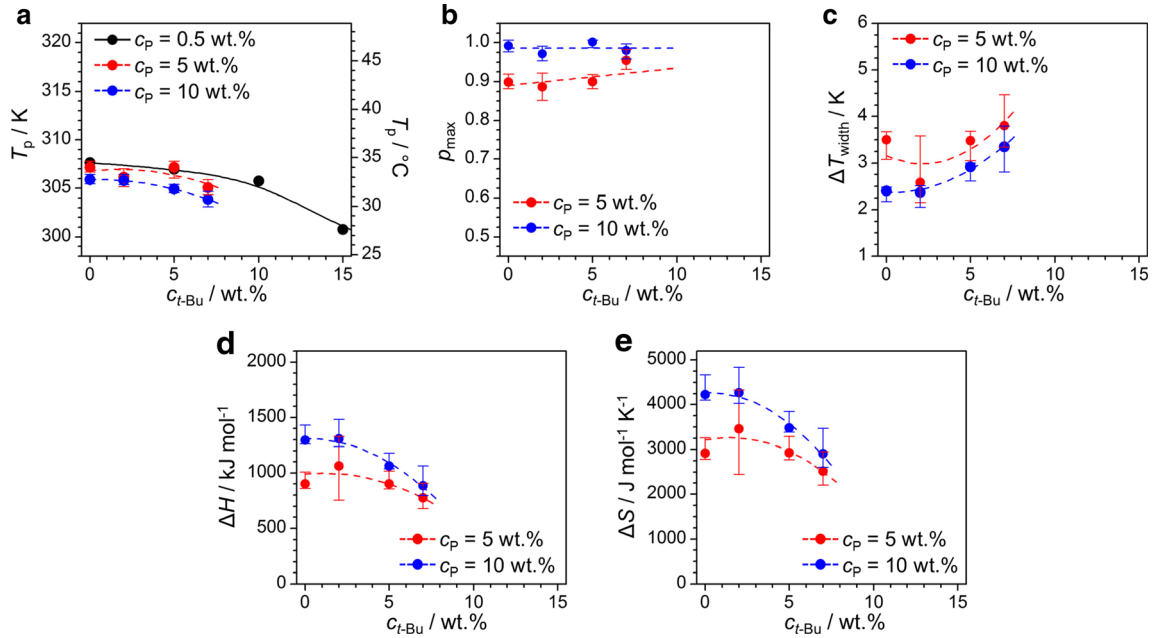

Fig. 4 Parameters characterizing phase separation of PVME as obtained from analysis of *p*-fractions in Fig. 2. **a** Phase separation temperatures T_p (values of T_p for c_P = 0.5 wt% are obtained from [34]). **b** Maximum fraction of phase-separated PVME units p_{max}. **c** Width of phase separation ΔT_{width}. **d**, **e** Standard (with respect to molar concentration of cooperative domains of PVME) enthalpy change ΔH and entropy change ΔS, respectively, associated with phase separation of PVME. Two PVME and four *t*-BuOH concentrations were analysed. The *error bars* (at confidence interval 2σ) are calculated from estimated errors in Fig. 2a, b using the Monte Carlo method with 5000 simulations for each set of data points (corresponding to particular PVME and *t*-BuOH concentration) in Fig. 2. There seems to be strong positive correlation between ΔH and ΔS (as seen in **d**, **e**) and rather weak correlation between these two parameters and p_{max}, which is also reflected by propagation of magnitude of error

(4) enthalpy change ΔH and (5) entropy change ΔS associated with phase separation. Figure 4a shows a slight decrease of T_p with an increasing PVME weight fraction. This is consistent with previous observations [12, 13] where up to ca. 15 wt% of PVME causes the T_p to decrease after which at 15 wt%, a minimum is reached, the first critical point on its bimodal phase diagram. The hydrophobic *t*-BuOH additive also decreases T_p due to its association with PVME which promotes overall hydrophobicity of PVME/*t*-BuOH adducts. Figure 4b indicates that a lower concentration of neat PVME (c_P = 5 wt%) has about 10% (p_{max} ~0.9) of inseparable units. The addition of *t*-BuOH increases the p_{max} value, indicating that originally inseparable PVME units (perhaps low molecular fractions due to high polydispersity index about 3) form hydrophobic complexes with *t*-BuOH, promoting their separation. The content of low molecular fractions up to 10-mer was estimated using Schulz–Zimm distribution for linear step-growth polymers to be about 6 wt% of the PVME sample. Therefore, the difference in p_{max} values of lower and higher PVME concentrations (Fig. 4b) can be at least partially explained by the polydispersity of the sample.

The width of phase separation for both studied PVME concentrations has increasing tendency upon addition of *t*-BuOH (Fig. 4c). Figure 4d, e shows decreasing enthalpy and entropy change upon addition of *t*-BuOH. Decrease of ΔH upon addition of *t*-BuOH is a consequence of the hydrophobic association of *t*-BuOH with PVME which partially expels hydrogen-bonded D_2O molecules from the vicinity of PVME. This process results in a lower number of hydrogen bonds between D_2O solvent molecules and the PVME monomeric units. Subsequently, less heat is necessary for breaking the hydrogen bonds and the formation of the globular state. A similar decrease of ΔS indicates that less energy (upon addition of *t*-BuOH) is redistributed into the conformational change of PVME units during phase separation.

In fact, standard enthalpy and entropy as obtained from NMR are standard with respect to the molar concentration of *cooperative domains* of PVME. PVME monomeric units contained in this domain exhibit cooperative phase separation in an 'all-or-none' manner [38–40]. One approach to estimate the number of monomeric units in the cooperative domain is to compare the ΔH as obtained from NMR and DSC (i.e. the ratio $\Delta H_{NMR}/\Delta H_{DSC}$). From [20], the ΔH_{DSC} values for systems with neat PVME (c_P = 5 wt%) and PVME with *t*-BuOH (c_P = 5 wt%, $c_{t\text{-Bu}}$ = 5 wt%) are 4050 and 2300 J mol^{-1}, respectively. This yields values of monomeric units in a cooperative domain around 220 (±18) and 390 (±36) for neat PVME (c_P = 5 wt%) and PVME with *t*-BuOH (c_P = 5 wt%, $c_{t\text{-Bu}}$ = 5 wt%). Therefore, the addition of *t*-BuOH apparently increases the size of the cooperative domain of PVME.

In order to probe the mobility of solvent molecules (both D_2O and *t*-BuOH) bound in globular structures of PVME above phase separation temperature T_p, time-resolved spin–spin ^{1}H NMR

relaxation experiments were performed. Values of spin–spin ^{1}H NMR relaxation time T_2 were obtained for residual CH_3 resonance (in *t*-BuOH at 1.15 ppm) and residual HDO (together with OH from *t*-BuOH at around 4.5 ppm) at 312 K (≈39 °C, above phase separation temperature). The system was monitored for up to 90 h (about 4 days). Relatively high T_2 values measured at the temperature 295 K (≈22 °C) below T_p clearly show a significant reduction of mobility of both solvent molecules (D_2O and *t*-BuOH) when the system passes T_p to a separated state. This is manifested as a decrease of T_2 for both HDO and CH_3 of *t*-BuOH resonance below (at 295 K) and above (at 312 K) T_p as seen in Table 1. This effect is more pronounced in samples with higher 10 wt% PVME content.

Low T_2 value of CH_3 resonance of *t*-BuOH at 312 K (≈39 °C) is gradually increasing with time, reaching value corresponding to *t*-BuOH in D_2O without PVME (see Fig. 5). Similar behaviour can be seen for HDO resonance. However, T_2s reach values even higher than those corresponding to HDO in neat *t*-BuOH/D_2O system. This is perhaps due to a complicated spin–spin relaxation mechanism where the chemical exchange between HDO, D_2O, H_2O and *t*-BuOH species has a strong effect on overall T_2 value.

Strong PVME concentration dependence of the T_2 time evolution is observed (compare Fig. 5a, b). Lower concentration (5 wt%) has an exponential-like increase of T_2 while higher (10 wt%) has a sigmoidal-like increase. The exponential-like dependency (5 wt% of PVME) might also have sigmoidal shape at very short times after phase separation; however, the experimental technique used does not allow to probe these timescales. Therefore, the fitted tendencies are used rather to guide the reader's eye. The time for reaching a plateau can be estimated as 20 and 60–120 h (2.5–5 days) for 5 and 10 wt% of PVME, respectively. The concentration of *t*-BuOH has only a minor effect for 5 wt% of PVME and relatively significant effect for 10 wt% of PVME. There is a direct connection between the time evolution of T_2 and the rate of the release of solvent molecules bound in globular structures of PVME. The observed relaxation rate ($R_{2obs} = 1/T_{2obs}$) can be expressed as a population-weighted sum of relaxation rates of free ($R_{2free} = 1/T_{2free}$) and bound

Table 1 ^{1}H NMR T_2 values for PVME (in 5 wt% *t*-BuOH in D_2O/*t*-BuOH solution) below and above phase separation temperature

	T_2/s			
	PVME concentration			
	5 wt%		10 wt%	
	Type of resonance			
Temperature (K)	HDO	CH_3 (*t*-BuOH)	HDO	CH_3 (*t*-BuOH)
295	1.0	1.7	0.9	1.6
312	0.38	1.47	0.16	0.8

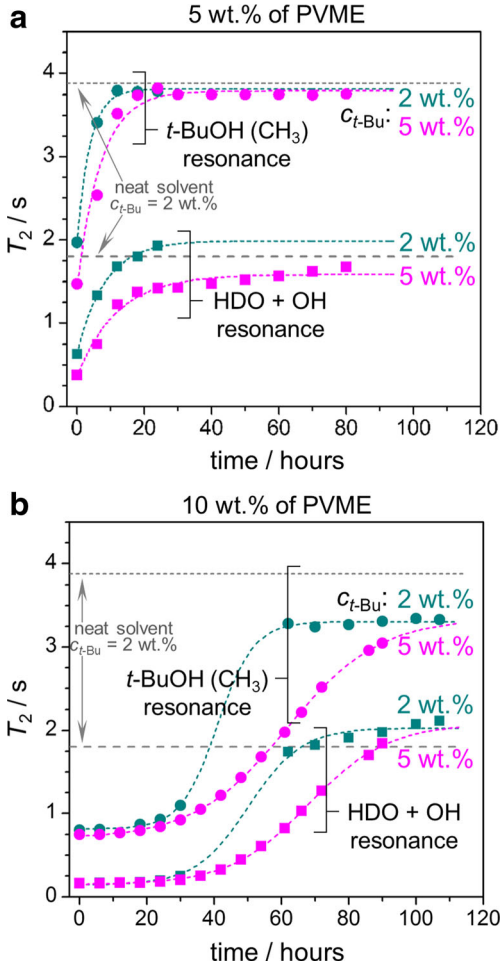

Fig. 5 Time-resolved spin–spin relaxation time T_2 of HDO + OH and CH_3 (of *t*-BuOH) resonances (see Fig. 1, resonances E and D) above phase separation temperature at 312 K (~39 °C). Data for **a** 5 wt% and **b** 10 wt% of PVME with two concentrations of binary solvent $c_{t\text{-Bu}}$ = 2 and 5 wt% are shown. Data are fitted (*cyan* and *magenta dashed lines*) with **a** exponential function and **b** sigmoidal function in order to guide the reader's eye. *Grey dashed lines* are values for neat binary solvent without presence of PVME

($R_{2bound} = 1/T_{2bound}$) solvent molecules (assuming fast exchange between these two states):

$$(T_{2obs})^{-1} = f_{bound}(T_{2bound})^{-1} + (1-f_{bound})(T_{2free})^{-1} \quad (8)$$

where f_{bound} is the fraction of solvent molecules bound within globular structures. f_{bound} is a time-dependent parameter—its first time derivative reflects the rate of release of solvent molecules from PVME separated structures. Unfortunately, we were not able to extract this value from our experiments which limits the interpretation. This is due to the fact that only one resonance corresponding to both bound and free solvent molecules was observed. Equation 8 is also constructed based on the assumption that there is no chemical exchange of protons between free and bound species or between the two types of solvent molecules (*t*-BuOH or D_2O). This condition apparently holds only for the relaxation of CH_3 groups in *t*-BuOH which are unexchangeable

(OH groups are exchangeable). Therefore, only the T_2 values for the CH_3 group (*t*-BuOH) are always below the upper limit defined by T_2 in neat *t*-BuOH/D_2O solvent (top dashed grey lines in Fig. 5a, b).

Nevertheless, Fig. 5 gives indirect information about the structure of the phase-separated PVME. Large differences in the behaviour of lower and higher concentrations of PVME indicate that solvent molecules are trapped in 'cavities' in collapsed globular-like structures and slowly released from them. The release time for each solvent molecule is somewhat proportional to the size of globular-like aggregate from which it escapes (for this model see Fig. 6). During this process, the aggregates become more compact. At 5 wt% of PVME, the aggregated structures are rather small and solvent molecules can readily escape (20 h). At 10 wt% of PVME, it seems that the aggregated structures form a sponge-like morphology with encapsulated solvent molecules, which needs more time to be completely released (60 to 120 h depending on *t*-BuOH concentration). The T_2 values of CH_3 of *t*-BuOH also indicate that almost all the *t*-BuOH molecules are released from globular structures at low PVME concentration (Fig. 5a) while at high PVME concentration, some *t*-BuOH remains in relatively strong contact with the surface of globular structures (Fig. 5b; the T_2 values of CH_3 group do not reach those of neat solvent). It seems that after 120 h, there are no detectable solvent molecules trapped inside the globules. Presence of trapped solvent would strongly change its chemical environment and lead to appearance of new peak in NMR spectrum (which was not observed).

ITC experiments were additionally conducted in order to monitor the interactions of PVME with *t*-BuOH at three defined temperatures: 306, 308 and 310 K, corresponding to non-separated, partially separated and fully separated state of PVME, respectively (Fig. 7a). Each experiment was performed by the sequential addition of *t*-BuOH stock solution ($c_{t\text{-Bu}}$ = 2 wt%, in H_2O) into PVME solution (c_P = 1 wt%, in neat H_2O). At temperatures below phase transition (306 K), the polymer is dissolved in a free-coil state, according to NMR data. The interactions between polymer and alcohol are characterized by a small exothermic effect, even smaller than during the dilution of pure *t*-BuOH stock solution in water (compare Fig. 7b, c). When the temperature of the experiment is adjusted to 310 K, above the transition temperature, the exothermic effect of the interaction becomes significantly larger (Fig. 7a). It is worth mentioning that the heating of the polymer solution was performed prior to adding alcohol. Therefore, the exothermic effect of the reaction can be attributed to an interaction of *t*-BuOH molecules with collapsed PVME structures. The non-presence of endothermic responses (possibly attributable to the simultaneous release of

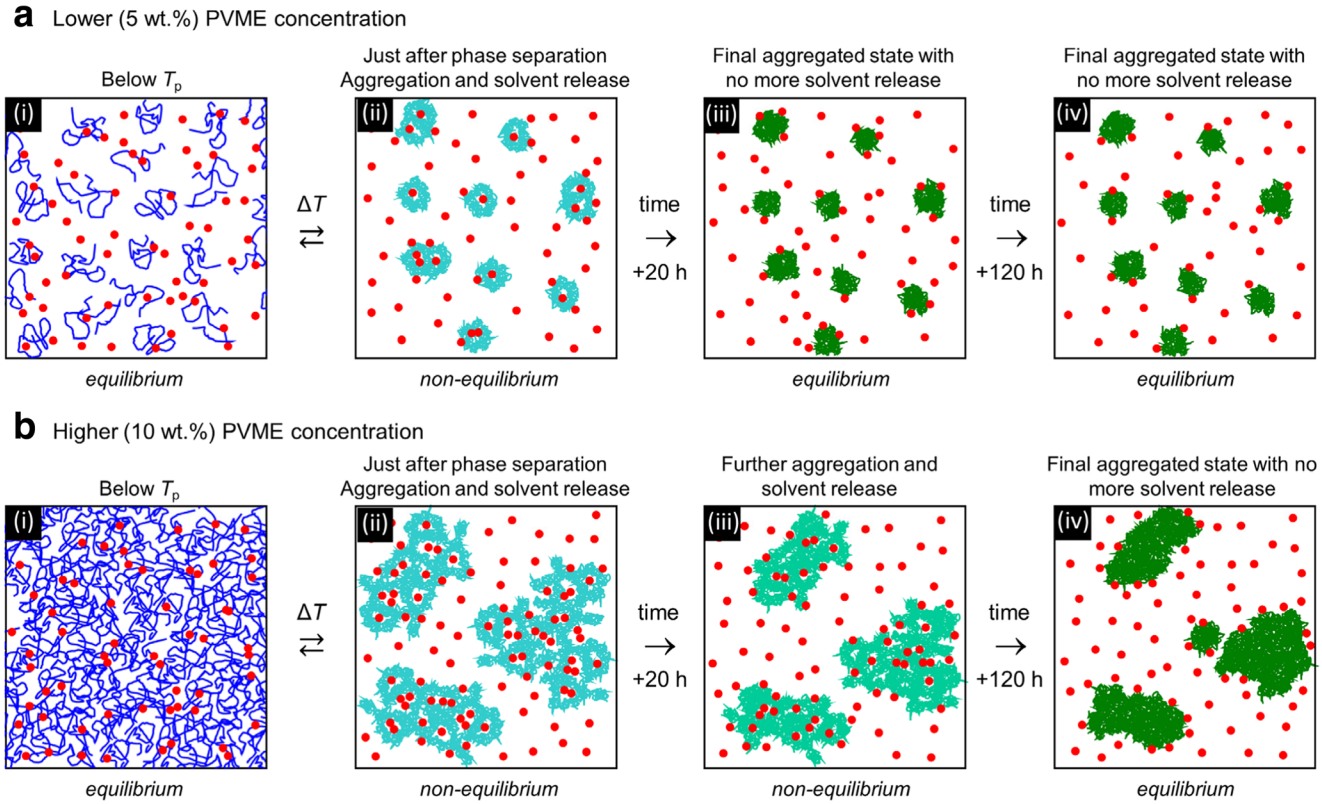

Fig. 6 Model of phase separation of PVME based on NMR relaxation measurements for **a** lower and **b** higher PVME concentrations. **a** Lower PVME concentration (*i*) after phase separation (*ii*) allows continuous release of solvent molecules, and within 20 h (*iii*), the process reaches its equilibrium with no further change (*iv*). **b** Higher PVME content (*i*) after phase separation forms non-equilibrium sponge-like structures (*ii*) with solvent molecules trapped inside. With time, the system slowly releases solvent (*iii*) and moves towards the equilibrium (*iv*)

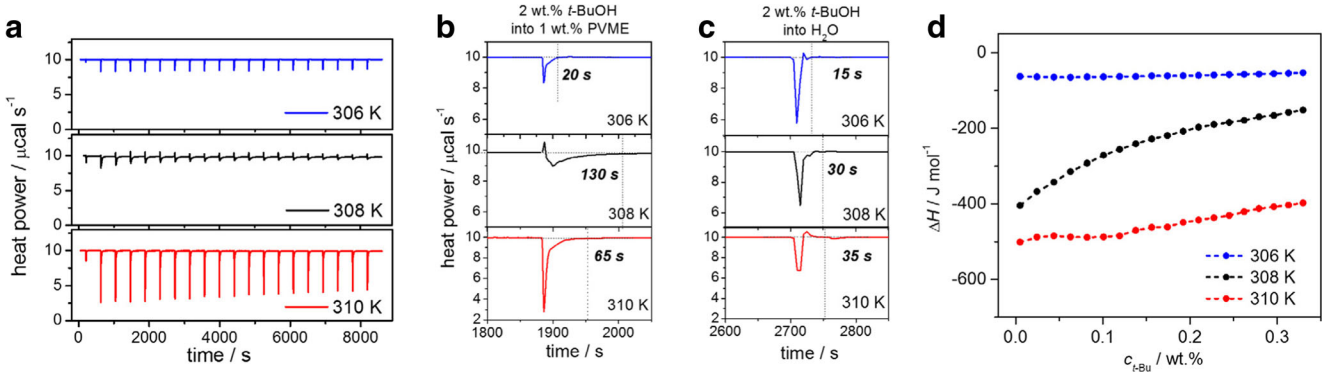

Fig. 7 ITC data for titration of *t*-BuOH stock solution ($c_{t\text{-Bu}}$ = 2 wt%, in H_2O) into PVME solution (c_P = 1 wt%, in neat H_2O) at different temperatures: 306, 308 and 310 K. **a** Raw ITC data obtained as a heat power delivered to measurement cell vs. time. **b** Magnification of one selected stock solution addition (into PVME solution, as seen in **a**) in order to emphasize the equilibration time. **c** Control experiment of *t*-BuOH stock solution ($c_{t\text{-Bu}}$ = 2 wt%, in H_2O) addition into neat water. **d** Plot of enthalpy change connected with *t*-BuOH/PVME interaction as a function of *t*-BuOH weight fraction

bound water) indicates an attraction between hydrophobic *t*-Bu groups of *t*-BuOH and PVME globular structure which takes place only on the surface of PVME compact structures (as indicated by NMR relaxation experiments).

Enthalpy changes as a function of the *t*-BuOH weight fraction are shown in Fig. 7d. At 308 and 310 K, they gradually decay towards a saturation value which indicates that *t*-BuOH hydrophobically interacts with the surface shell of PVME globular structures. NMR relaxation experiments support this idea since the mobility of *t*-BuOH is high (above T_p and after long time period); i.e. there are no strongly bound *t*-BuOH molecules.

Meanwhile, the most intriguing result was obtained at 308 K, where dual exothermic/endothermic effects and kinetics in a time range of a couple of minutes were observed (Fig. 7a, b). By taking into account the two facts mentioned earlier (i.e. the relation of endothermic effect with bound water release and rapid dehydration of PVME chains at low PVME concentration above phase separation temperature), two contributions to the interaction mechanism at 308 K can be expected. The addition of *t*-BuOH results in an almost simultaneous release of bound water out of the polymer chains with a subsequent interaction of hydrophobic parts of *t*-BuOH and PVME. Moreover, both of these processes possess a relatively slow dynamic to be able to appear with an equilibration time about 130 s during the ITC measurement (equilibration time is time needed for a system to recover from min/max of heating power to the baseline level).

Conclusions

NMR and ITC techniques were chosen to examine interactions between PVME polymer and solvent molecules (D_2O and *t*-BuOH additive). The presence of small amounts of *t*-BuOH lowers the phase separation temperature and also makes the separation wider (onset and offset temperatures are further apart). A maximum fraction of phase-separable PVME units (p_{max}) increases with PVME concentration as well as with *t*-BuOH concentration. Therefore, the presence of the *t*-BuOH additive increases the overall hydrophobicity of PVME. Thermodynamic parameters connected with phase separation were calculated from NMR results using an approach based on the van't Hoff equation. This revealed that the *t*-BuOH presence increases the number of PVME monomeric units in one cooperative domain (where all monomeric units undergo phase separation as whole—'all-or-none'). NMR time-resolved relaxation measurements show a different dynamic of the solvent releasing process for low and high PVME concentrations (above phase separation temperature). The concentration-dependent morphology of PVME is the key factor determining the time period for the release of solvent molecules. ITC data indicate that the addition of *t*-BuOH molecules results in decrease of PVME solvation by water molecules, in agreement with NMR results (*t*-BuOH lowers phase separation temperature). ITC also suggests that *t*-BuOH interacts strongly with only the surface shell of PVME globular structures through the attraction of hydrophobic domains of PVME and *t*-BuOH components above phase separation temperature. The presented results on the PVME/*t*-BuOH/D_2O system indicate that the PVME solution properties are *not* constant in time and the analysis of measurements (and resulting properties) should always be done with consideration of this strong time-dependent behaviour.

Acknowledgements This work was supported by the World Premier International Research Initiative (WPI Initiative), Ministry of Education, Culture, Sports, Science and Technology (MEXT), Japan and the Grant Agency of the Academy of Science of the Czech Republic (Grant No. 15-10527 J). The authors also acknowledge the Charles University, Prague for the opportunity for N. Velychkivska's doctoral studies.

Compliance with ethical standards

Conflict of interest The authors declare that they have no competing financial interest.

References

1. Aseyev V, Tenhu H, Winnik FM (2006) Temperature dependence of the colloidal stability of neutral amphiphilic polymers in water. Adv Polym Sci 196:1–85
2. Liu R, Fraylich M, Saunders BR (2009) Thermoresponsive copolymers: from fundamental studies to applications. Colloid Polym Sci 287:627–643
3. Jeong B, Gutowska A (2002) Lessons from nature: stimuli-responsive polymers and their biomedical applications. Trends Biotechnol 20:305–311
4. Ward MA, Georgiou TK (2011) Thermoresponsive polymers for biomedical applications. Polymers 3:1215–1242
5. Alarcon CDH, Pennadam S, Alexander C (2005) Stimuli responsive polymers for biomedical applications. Chem Soc Rev 34:276–285
6. Jochum FD, Theato P (2013) Temperature- and light-responsive smart polymer materials. Chem Soc Rev 42:7468–7483
7. Schild HG, Tirrell DA (1990) Microcalorimetric detection of lower critical solution temperatures in aqueous polymer solutions. J Phys Chem 94:4352–4356
8. Heskins M, Guillet JE, James EJ (1968) Solution properties of poly(N-isopropylacrylamide). J Macromol Sci Chem A2:1441–1455
9. Schild HG (1992) Poly(N-isopropylacrylamide): experiment, theory and application. Prog Polym Sci 17:163–249
10. Chen G, Hoffman AS (1995) Graft copolymers that exhibit temperature-induced phase transition over a wide range of pH. Nature 373:49–52
11. De Rossi D, Kajiwara K, Osada Y, Yamadin A (1991) Polymer gels fundamentals and biomedical applications. Plenum Press, New York
12. Schäfer-Soenen H, Moerkerke R, Berghmans H, Koningsveld R, Dušek K, Šolc K (1997) Zero and off-zero critical concentrations in systems containing polydisperse polymers with very high molar masses. 2. The system water-poly(vinyl methyl ether). Macromolecules 30:410–416
13. Swier S, Van Durme K, Van Mele B (2003) Modulated-temperature differential scanning calorimetry study of temperature-induced mixing and demixing in poly(vinylmethylether)/water. J Polym Sci Part B Polym Phys 41:1824–1836
14. Maeda H (1994) Interaction of water with poly(vinyl methyl ether) in aqueous solution. J Polym Sci Part B Polym Phys 32:91–97
15. Spěváček J, Hanyková L, Starovoytova L (2004) ^{1}H NMR relaxation study of thermotropic phase transition in poly(vinyl methyl ether)/D_2O solutions. Macromolecules 37:7710–7718
16. Hanyková L, Labuta J, Spěváček J (2006) Effect of time on the hydration and temperature-induced phase separation in aqueous polymer solutions. ^{1}H NMR study. Polymer 47:6107–6116
17. Labuta J, Hill JP, Hanyková L, Ishihara S, Ariga KJ (2010) Probing the microphase separation of thermoresponsive amphiphilic polymer in water/ethanol solution. Nanosci Nanotechol 10:8408–8416
18. Spěváček J, Hanyková L (2005) ^{1}H NMR study on the hydration during temperature-induced phase separation in concentrated poly(-vinyl methyl ether)/D_2O solutions. Macromolecules 38:9187–9191
19. Starovoytova L, Spěváček J (2006) Effect of time on the hydration and temperature-induced phase separation in aqueous polymer solutions. ^{1}H NMR study. Polymer 47:7329–7334
20. Starovoytova L, Št'astná J, Šturcová A, Konefal R, Dybal J, Velychkivska N, Radecki M, Hanyková L (2015) Additive effects on phase transition and interactions in poly (vinyl methyl ether) solutions. Polymers 7:2572–2583
21. Spěváček J, Dybal J (2011) Stimuli-responsive polymers in solution investigated by NMR and infrared spectroscopy. Macromol Symp 303:17–25
22. Hanyková L, Spěváček J, Ilavský M (2001) ^{1}H NMR study of thermotropic phase transition of linear and crosslinked poly(vinyl methyl ether) in D_2O. Polymer 42:8607–8612
23. Maeda Y (2001) IR spectroscopic study on the hydration and the phase transition of poly(vinyl methyl ether) in water. Langmuir 17:1737–1742
24. Zeng XG, Yang XZ (2004) A study of interaction of water and model compound of poly(vinyl methyl ether). J Phys Chem B 108:17384–17392
25. Van Durme K, Loozen E, Nies E, Van Mele B (2005) Phase behavior of poly(vinyl methyl ether) in deuterium oxide. Macromolecules 38:10234–10243
26. Zhang WZ, Chen XD, Luo WA, Yang J, Zhang MQ, Zhu FM (2009) Study of phase separation of polyvinyl methyl ether aqueous solutions with rayleigh scattering technique. Macromolecules 42:1720–1725
27. Meeussen F, Bauwens Y, Moerkerke R, Nies ELF, Berghmans H (2000) Molecular complex formation in the system poly(vinyl methyl ether)/water. Polymer 41:3737–3743
28. Pastorczak M, Kozanecki M, Ulanski J (2009) Water-polymer interactions in PVME hydrogels—Raman spectroscopy studies. Polymer 50:4535–4542
29. Hofmann C, Schönhoff M (2012) Dynamics and distribution of aromatic model drugs in the phase transition of thermoreversible poly(N-isopropyl acrylamide) in solution. Colloid Polym Sci 290:689–698
30. Maeda Y, Mochiduki H, Yamamoto H, Nishimura Y, Ikeda I (2003) Effects of ions on two-step phase separation of poly(vinyl methyl ether) in water as studied by IR and Raman spectroscopy. Langmuir 19:10357–10360
31. Karlström G, Carlsson A, Lindman B (1990) Phase diagrams of nonionic polymer-water systems. Experimental and theoretical studies of the effects of surfactants and other cosolutes. J Phys Chem 94:5005–5015
32. Zhang YJ, Furyk S, Bergbreiter DE, Cremer PS (2005) Specific ion effects on the water solubility of macromolecules: PNIPAM and the Hofmeister series. J Am Chem Soc 127:14505–14510
33. Horne RA, Almeida JP, Day AF, Yu NT (1971) Macromolecule hydration and the effect of solutes on the cloud point of aqueous solutions of polyvinyl methyl ether: a possible model for protein denaturation and temperature control in homeothermic animals. J Colloid Interface Sci 35:77–84
34. Maeda Y, Yamamoto H, Ikeda I (2004) Micro-Raman spectroscopic investigation on the phase separation of poly(vinyl methyl ether)/alcohol/water ternary mixtures. Langmuir 20:7339–7341
35. Prasad M, Moulik SP, Wardian AA, Moore S, Van Bommel A, Palepu R (2005) Alkyl (C10, C12, C14 and C16) triphenyl phosphonium bromide influenced cloud points of nonionic surfactants (Triton X 100, Brij 56 and Brij 97) and the polymer (polyvinyl methyl ether). Colloid Polym Sci 283:887–897
36. Hofmann C, Schönhoff M (2009) Do additives shift the LCST of poly(N-isopropyl acrylamide) by solvent quality changes or by direct interactions? Colloid Polym Sci 287:1369–1376
37. Spěváček J, Hanyková L (2007) NMR study on polymer-solvent interactions during temperature-induced phase separation in aqueous polymer solutions. Macromol Symp 251:72–80
38. Tiktopulo EI, Uversky VN, Lushchik VB, Klenin SI, Bychkova VE, Ptitsyn OB (1995) "Domain" coil-globule transition in homopolymers. Macromolecules 28:7519–7524
39. Tiktopulo EI, Bychkova VE, Ricka J, Ptitsyn OB (1994) Cooperativity of the coil-globule transition in a homopolymer: microcalorimetric study of poly(N-isopropylacrylamide). Macromolecules 27:2879–2882
40. Hanyková L, Radecki M (2012) NMR and thermodynamic study of phase transition in aqueous solutions of thermoresponsive amphiphilic polymer. Chem Lett 41:1044–1046

Nadiia Velychkivska received her BSc and MSc from Lviv Polytechnic National University in the field of chemical technology of fuel and carbon materials in 2012. In 2013, she joined the Department of NMR Spectroscopy at the Institute of Macromolecular Chemistry, Prague. As a UNESCO/IUPAC student, she worked with temperature-sensitive polymers. Since 2014, Ms. Velychkivska has been a PhD student and her overall scientific interest lies in the investigation of temperature-sensitive macromolecular and supramolecular systems by means of high-resolution NMR spectroscopy, which can be used in drug delivery, cosmetics or photodynamic therapy.

Anna Bogomolova received her B.Sc. and M.Sc. in Polymer Chemistry from the Saint-Petersburg State University, Russia. She completed her Ph.D. in Physical Chemistry in 2015 at the Institute of Macromolecular Chemistry, Prague. After a 1-year postdoctoral fellowship under the supervision of Prof. Helmut Schlaad at the Max Planck Institute of Colloids and Interfaces in Potsdam, she moved back to Prague, where she has been currently working as a postdoctoral researcher.

Sergey K. Filippov received a B.S., M.Sc. with honours and Ph.D. in polymer physics from the University of Saint-Petersburg, Russia. His Ph.D. thesis was devoted to polymeric liquid crystals. During his Ph.D. studies he spent 1 year in Oxford University in the group of Prof. Steve Elston. Between 1999 and 2001, he was employed as a postdoctoral researcher at Puerto Rico University. In 2002, he re-joined the Saint-Petersburg State University as an assistant professor. In 2007, he joined the Institute of Macromolecular Chemistry in Prague, Czech Republic, as a research scientist in the Department of Supramolecular Polymer Systems, headed by Petr Štěpánek. In 2014, he became a senior research scientist in the same department. Dr. Filippov's main research interests are dynamic light scattering, small-angle X-ray and neutron scattering and isothermal titration calorimetry in application to self-assembling systems in soft matter.

Larisa Starovoytova is a research fellow at NMR spectroscopy laboratory, Institute of Macromolecular Chemistry, Prague, Czech Republic. She received her PhD in Biophysics and Macromolecular Physics from Charles University in Prague. Research experiences: spectroscopic methods (NMR, infrared, SANS spectroscopy, NMR fast-field-cycling relaxometry), phase separation in polymer systems, structural and dynamical changes and complex formation during phase transition and influence of the structure and interactions on phase behaviour of temperature-sensitive polymers.

Jan Labuta received a Ph.D. (2008) from Charles University, Prague, Czech Republic. He was awarded a JSPS postdoctoral fellowship to perform research at Supermolecules Group (SMG), National Institute for Materials Science (NIMS), Tsukuba, Japan, and continued his work there as an research associate of the International Center for Materials Nanoarchitectonics (MANA), NIMS. Then, he took a position as independent postdoctoral researcher at the International Centre for Young Scientists (ICYS), NIMS. From 2016, he holds permanent position as MANA Independent Scientist (senior researcher) at MANA, NIMS. His research interests are host–guest and supramolecular chemistry, chemical equilibria, sensing, chirality, tautomerism and phase separation phenomenon of stimuli-responsive polymers and/or porphyrin derivatives.

Publication № 3

ACS OMEGA

Article

Cite This: ACS Omega 2018, 3, 11865−11873

http://pubs.acs.org/journal/acsodf

Improving the Colloidal Stability of Temperature-Sensitive Poly(*N*-isopropylacrylamide) Solutions Using Low Molecular Weight Hydrophobic Additives

Nadiia Velychkivska,[†] Larisa Starovoytova,[†] Václav Březina,[‡] Lenka Hanyková,[‡] Jonathan P. Hill,*[,§] and Jan Labuta*[,§]

[†]Department of NMR Spectroscopy, Institute of Macromolecular Chemistry AS CR, v.v.i., Heyrovsky Sq. 2, Prague 6 162 06, Czech Republic

[‡]Faculty of Mathematics and Physics, Department of Macromolecular Physics, Charles University, V Holešovičkách 2, 180 00 Prague 8, Czech Republic

[§]National Institute for Materials Science (NIMS), International Center for Materials Nanoarchitectonics (WPI-MANA), 1-1 Namiki, Tsukuba, Ibaraki 305-0044, Japan

ABSTRACT: Poly(*N*-isopropylacrylamide) (PNIPAM) is an important polymer with stimuli-responsive properties, making it suitable for various uses. Phase behavior of the temperature-sensitive PNIPAM polymer in the presence of four low-molecular weight additives *tert*-butylamine (*t*-BuAM), *tert*-butyl alcohol (*t*-BuOH), *tert*-butyl methyl ether (*t*-BuME), and *tert*-butyl methyl ketone (*t*-BuMK) was studied in water (D_2O) using high-resolution nuclear magnetic resonance (NMR) spectroscopy and dynamic light scattering. Phase separation was thermodynamically modeled as a two-state process which resulted in a simple curve which can be used for fitting of NMR data and obtaining all important thermodynamic parameters using simple formulas presented in this paper. The model is based on a modified van't Hoff equation. Phase separation temperatures T_p and thermodynamic parameters (enthalpy and entropy change) connected with the phase separation of PNIPAM were obtained using this method. It was determined that T_p is dependent on additives in the following order: T_p(*t*-BuAM) > T_p(*t*-BuOH) > T_p(*t*-BuME) > T_p(*t*-BuMK). Also, either increasing the additive concentration or increasing pK_a of the additive leads to depression of T_p. Time-resolved ^{1}H NMR spin−spin relaxation experiments (T_2) performed above the phase separation temperature of PNIPAM revealed high colloidal stability of the phase-separated polymer induced by the additives (relative to the neat PNIPAM/D_2O system). Small quantities of selected suitable additives can be used to optimize the properties of PNIPAM preparations including their phase separation temperatures, colloidal stabilities, and morphologies, thus improving the prospects for the application.

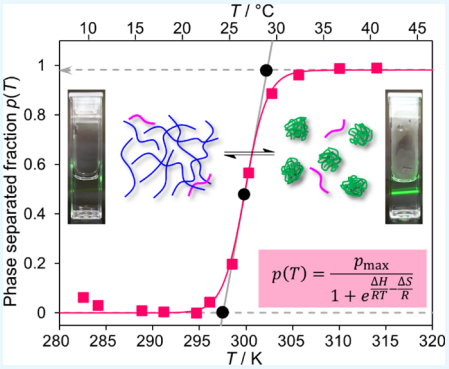

1. INTRODUCTION

Stimuli-responsive polymers, also called "smart polymers", are a group of materials which are responsive to external stimuli due to variations in their hydrophilic−hydrophobic characters.[1−5] Temperature, solvents, salts, pH, electromagnetic radiation, chemical, or biological agents are all potential stimuli which can trigger a response,[1,5−7] and there are also a variety of responses, including conformational change, micelle formation, dissolution/precipitation, or variations in optical or electrical properties. Temperature-responsive polymers are well-known for their unique property to undergo phase separation upon temperature decrease (upper critical solution temperature behavior—UCST) or temperature increase (lower critical solution temperature behavior—LCST).[7−16] The phenomenon of phase separation is due to a coil−globule transition, whereby the expanded coils of polymer chains undergo a transition to compact polymer globules. At the molecular level, phase separation in solutions is considered to be a macroscopic manifestation of a coil−globule transition followed by further aggregation and formation of colloidally stable mesoglobules.[4,17,18] Phase separation is associated with variations in the balance between several types of interactions, including hydrogen bonds and hydrophobic interactions.[4] Prolonging the colloidal stability of phase-separated polymers is an important issue in applications such as controlled release, drug delivery, bioseparation, and diagnostics. It is still unclear, for some polymers, what is the main driving force behind their high colloid stability in thermodynamically unfavorable media.[4]

Poly(*N*-isopropylacrylamide) (PNIPAM) is a well-known temperature-responsive polymer with LCST at approximately 32 °C,[19] close to human body temperature. This makes PNIPAM-based systems interesting for various biomedi-

Received: July 30, 2018
Accepted: September 11, 2018
Published: September 25, 2018

cal[1,2,6,7,20−26] and technological[8] applications. PNIPAM and its copolymers have been widely studied by means of light-scattering techniques,[19,27] Fourier transform infrared spectroscopy,[3,28] refractometry,[29] pressure perturbation calorimetry,[30] differential scanning calorimetry,[31−33] isothermal titration calorimetry,[34] and nuclear magnetic resonance (NMR) spectroscopy.[10,27,28,33,35,36] The presence of low-molecular weight compounds such as salts[37] or surfactants[38] can shift the phase equilibrium of PNIPAM to higher or lower temperatures. PNIPAM can also undergo phase separation at a constant temperature by changing the ratio of two polar solvents (e.g., water−methanol, water−ethanol, and water−tetrahydrofuran), the so-called co-nonsolvency effect.[15,39,40] These properties make PNIPAM attractive for various applications.

In this work, we provide a comparative analysis of the effects of low-molecular weight hydrophobic additives on the phase separation of PNIPAM. In particular, the behavior of PNIPAM in response to small quantities of *tert*-butyl alcohol (*t*-BuOH), *tert*-butylamine (*t*-BuAM), *tert*-butyl methyl ether (*t*-BuME), and *tert*-butyl methyl ketone (*t*-BuMK) additives has been investigated (Figure 1). NMR spectroscopy was used as the

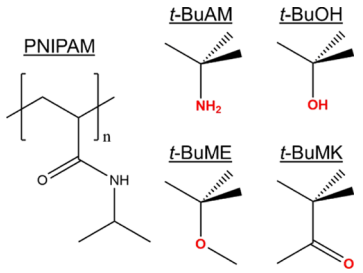

Figure 1. Chemical structures of temperature-sensitive PNIPAM and the additives used in this study: *tert*-butylamine (*t*-BuAM), *tert*-butyl alcohol (*t*-BuOH), *tert*-butyl methyl ether (*t*-BuME), and *tert*-butyl methyl ketone (*t*-BuMK).

main technique for the analysis of the effects of additives on phase behavior with phase separation being modeled as a two-state dynamical process. The NMR data were rationalized in terms of a modified van't Hoff equation fitted to experimental data. This approach allows determination of thermodynamic parameters such as the variations in enthalpy and entropy associated with phase separation. ^{1}H NMR spin−spin relaxation experiments (T_2) were used to examine the molecular mobility of the additives and D_2O solvent molecules. Spin−spin relaxation times T_2 provide information about the colloidal stability of phase-separated PNIPAM over time. The dynamic light scattering (DLS) technique was used to determine the sizes of polymer globules formed above the phase separation temperature.

2. RESULTS AND DISCUSSION

Examples of NMR spectra of PNIPAM (5 wt % in D_2O) in the presence of the additives studied (2 wt % in D_2O) below (22 °C) and above (~41 °C) the phase separation temperature are shown in Figure 2. The spectra clearly indicate that after phase separation, the resonances due to PNIPAM (a, b, c, and d resonances in Figure 2) disappear. This effect is connected with the low mobility of PNIPAM globular structures above phase separation.

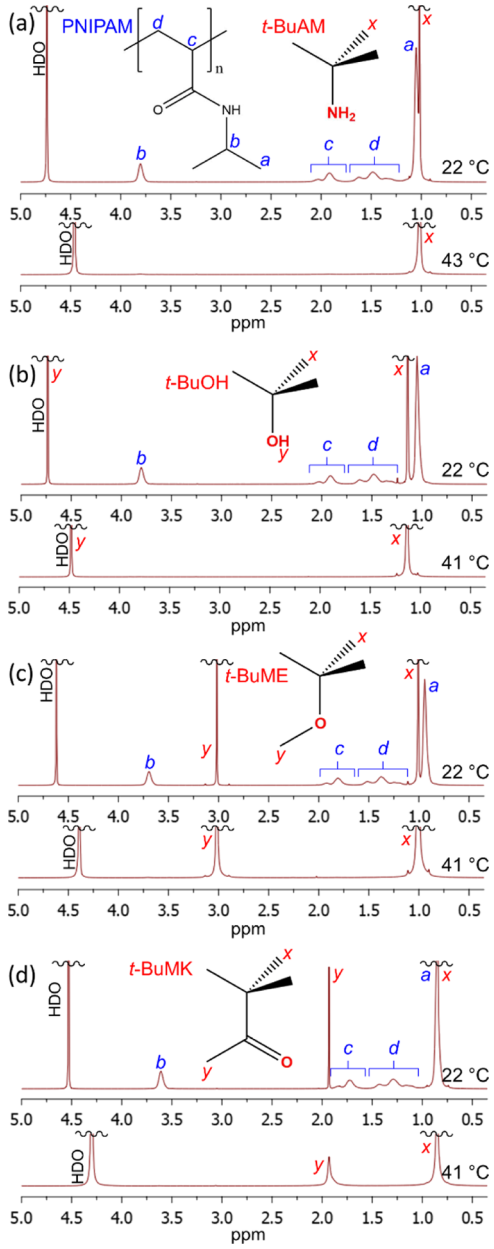

Figure 2. ^{1}H NMR (600.2 MHz) of PNIPAM (w_P = 5 wt %, D_2O) below (at 22 °C) and above (at ca. 41 °C) the phase separation temperature in the presence of $w_{additive}$ = 2 wt % of additives: (a) *t*-BuAM, (b) *t*-BuOH, (c) *t*-BuME, and (d) *t*-BuMK. Resonance assignments of PNIPAM and all additives are also shown for each case.

Figure 3a shows the ^{1}H NMR spectra measured during heating at small temperature steps either side of the phase separation temperature. A gradual decrease in the resonance intensity due to PNIPAM can be observed. To perform the quantitative analyses of the phase separation, the value of the phase-separated fraction of PNIPAM units $p(T)$ was calculated using the following formula.[10,41−43]

$$p(T) = 1 - \frac{I'(T)}{I'_0(T_0)} = 1 - \frac{T}{T_0}\frac{I(T)}{I_0(T_0)} \quad (1)$$

where $I'_0(T_0)$ is temperature-dependent integrated intensity of the NMR resonance corresponding to polymers below the phase separation temperature (usually determined at T_0 = 20

DOI: 10.1021/acsomega.8b01811
ACS Omega 2018, 3, 11865−11873

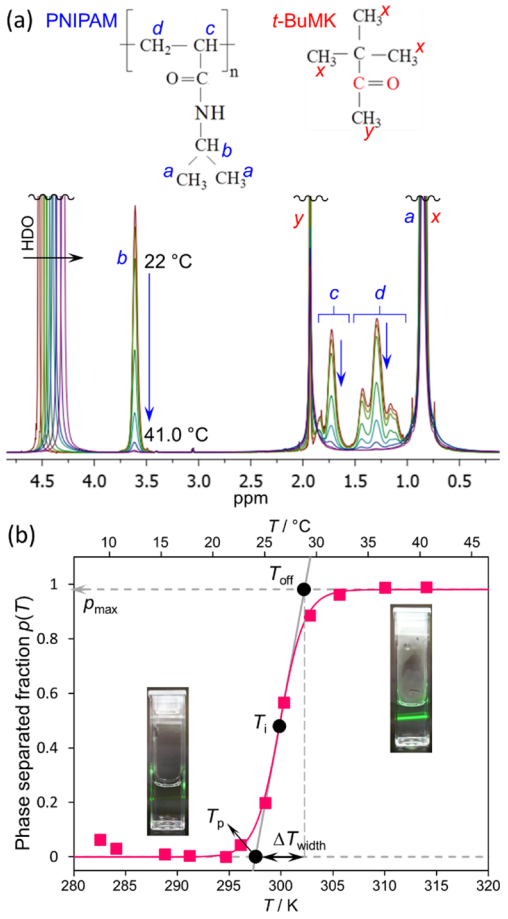

Figure 3. (a) Superimposed ^{1}H NMR (600.2 MHz) spectra of PNIPAM (w_p = 5 wt %) with *t*-BuMK additive ($w_{t\text{-BuMK}}$ = 2 wt %) measured at temperatures about the phase separation temperature. Assignment of PNIPAM and *t*-BuMK signals is shown. (b) Phase separation fraction $p(T)$ of PNIPAM polymer units (solid squares) as obtained from (a) using eq 1. The solid line is fit based on eq 6. Photos of solutions below and above phase separation (irradiated by a green laser pointer) are included.

°C). The $I'(T)$ is temperature-dependent integrated intensity of the same resonance in the partly phase-separated system (determined at T > 20 °C). The $I_0'(T_0)$ and $I'(T)$ values are unaffected by the fundamental temperature dependence of integrated intensities according to the Boltzmann equation. The Boltzmann equation states that the integrated intensities are temperature-dependent and decrease with absolute temperature as $1/T$. This effect is corrected in eq 1 using the formulae $I(T) = I'(T)/T$ and $I_0(T_0) = I0'(T_0)/T_0$, where $I(T)$ and $I_0(T_0)$ are Boltzmann-uncorrected integrated intensities as obtained from measurement of the partly phase-separated system and prior to phase separation, respectively. The "*b*" resonance corresponding to the NCH group of PNIPAM (Figure 3a) was used for evaluation of the integrated intensities and subsequent calculation of the phase-separated fraction. This yields the right side of eq 1 used for data analysis at temperatures $T \geq T_0$, where T is the actual temperature of measurement and T_0 is the temperature below phase separation of PNIPAM. The results obtained using this method are plotted in Figure 3b (solid squares).

To extract the thermodynamic parameters of the phase separation of PNIPAM solutions from NMR data, we have used a simple model based on two exchangeable states[41] (Figure 4). State one consists of polymer units in the coil form (a freely moving polymer chain). The second consists of

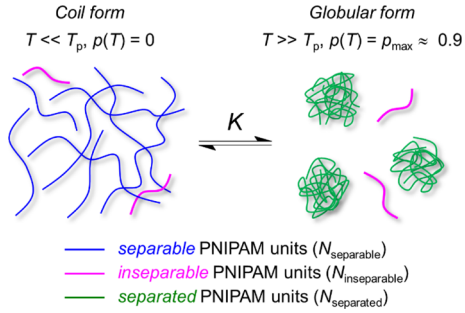

Figure 4. Schematic model of phase separation of the PNIPAM polymer containing three types of units used for the thermodynamic model.

polymer units in the globular form (rather compact rigid structures). The transition between these two states (coil–globule transition) is described by an equilibrium constant K, which is defined as the ratio of separated $N_{separated}$ and separable (but not separated yet) $N_{separable}$ PNIPAM units.

$$K = \frac{N_{separated}}{N_{separable}} \quad (2)$$

This model also takes into account that some polymer chains are not separable and remain in a coil state even at high temperatures (often attributed to the low molecular weight fractions of the polymer[44]), reflected by $N_{inseparable}$ (i.e., number of inseparable PNIPAM units). The fraction of phase-separated PNIPAM units $p(T)$ is generally defined in eq 3.

$$p(T) = \frac{N_{separated}}{N_{separable} + N_{inseparable} + N_{separated}} \quad (3)$$

The combination of eqs 2 and 3 gives a formula for $p(T)$ as a function of the equilibrium constant K

$$p(T) = \frac{p_{max}}{1 + K^{-1}} \quad (4)$$

where $p_{max} = (N_{separable} + N_{separated})/(N_{separable} + N_{inseparable} + N_{separated})$ is the maximum fraction of PNIPAM phase separable units. The van't Hoff equation for the temperature dependence of the equilibrium constant K is shown in eq 5.

$$K = e^{-(\Delta H - T\Delta S)/RT} \quad (5)$$

where ΔH and ΔS are the standard changes in enthalpy and entropy, respectively, connected with phase separation of PNIPAM. R is the gas constant (8.314 J mol^{-1} K^{-1}) and T is the absolute temperature. Combining eqs 4 and 5 yields a final formula for $p(T)$[41]

$$p(T) = \frac{p_{max}}{1 + e^{\Delta H/RT - \Delta S/R}} \quad (6)$$

Experimental data for $p(T)$ as shown in Figure 3b were fitted using eq 6 such that values of ΔH and ΔS could be obtained. Another important parameter is the temperature of the phase separation T_p, calculated as the onset temperature obtained from fitting of the $p(T)$ curve (see Figure 3b). The value of T_p is found at the intersection point of the tangent at the inflexion point T_i of the $p(T)$ curve and the x-axis. The inflexion is at the

DOI: 10.1021/acsomega.8b01811
ACS Omega 2018, 3, 11865−11873

point where the second derivative of $p(T)$ is zero $p''(T) = d^2p(T)/dT_2 = 0$, resulting in the following eq 7

$$2T_i(1 + e^{\Delta H/RT_i - \Delta S/R}) + \frac{\Delta H}{R}(1 - e^{\Delta H/RT_i - \Delta S/R}) = 0 \quad (7)$$

This equation does not have analytical solution in the closed form. Therefore, the numerical bisection method can be used for the determination of the inflexion point T_i. However, a solution of excellent accuracy can be found using an approximation. Equation 7 can be rearranged as eq 8.

$$\frac{2RT_i}{\Delta H} = \frac{e^{\Delta H/RT_i - \Delta S/R} - 1}{e^{\Delta H/RT_i - \Delta S/R} + 1} = \tanh\left[\frac{1}{2}\left(\frac{\Delta H}{RT_i} - \frac{\Delta S}{R}\right)\right] \approx \frac{1}{2}\left(\frac{\Delta H}{RT_i} - \frac{\Delta S}{R}\right) \quad (8)$$

where the term containing exponentials corresponds to the tanh function, subsequently approximated using the first term of its Taylor expansion (i.e., $\tanh(x) \approx x$). This yields a quadratic equation for T_i, eq 9

$$4R^2T_i^2 + \Delta H\Delta ST_i - \Delta H^2 = 0 \quad (9)$$

whose solution has the form of eq 10.

$$T_i = \frac{\Delta H\Delta S}{8R^2}\left(\sqrt{1 + \left(\frac{4R}{\Delta S}\right)^2} - 1\right) \quad (10)$$

At this point, the Taylor expansion of the square root up to the second order term is used (i.e., $\sqrt{1+x} \approx 1 + \frac{1}{2}x - \frac{1}{8}x^2$). After several rearrangements, a simple formula for the temperature at the inflexion point T_i can be obtained.

$$T_i = \frac{\Delta H}{\Delta S}\left(1 - \frac{4R^2}{\Delta S^2}\right) \quad (11)$$

The condition for the intersection of the tangent line at the inflexion point and x-axis leads to an expression for the temperature of phase separation T_p.

$$T_p = -\frac{p(T_i) - p'(T_i) \times T_i}{p'(T_i)} = T_i - \frac{RT_i^2}{\Delta H}(1 + e^{-\Delta H/RT_i + \Delta S/R}) \quad (12)$$

where $p'(T_i)$ denotes the first derivative of $p(T)$ with respect to T evaluated at T_i. Using a similar approach, an equation for the offset temperature T_{off} (Figure 3b) can be derived from the intersection of the tangent line with line $y = p_{max}$.

$$T_{off} = \frac{p_{max} - p(T_i) + p'(T_i) \times T_i}{p'(T_i)} = T_i + \frac{RT_i^2}{\Delta H}(1 + e^{\Delta H/RT_i - \Delta S/R}) \quad (13)$$

The offset temperature T_{off} indicates the point at which phase separation is nearly complete. From T_p and T_{off}, the width of the phase separation ΔT_{width} (the difference between offset and onset temperatures; see Figure 3b) can be determined using the following formula

$$\Delta T_{width} = T_{off} - T_p = \frac{2RT_i^2}{\Delta H}\left[1 + \cosh\left(\frac{\Delta H}{RT_i} - \frac{\Delta S}{R}\right)\right] \quad (14)$$

The fitting of experimental data using eq 6 yields values for ΔH, ΔS, and p_{max}. Thereafter, the parameters T_p and ΔT_{width} can be determined using eqs 12 and 14, respectively. Error analysis indicates that these approximations introduce only negligible errors into the values of T_i, T_p, T_{off}, and ΔT_{width} obtained.[a]

Figure 5 shows $p(T)$ as calculated from NMR experimental data for samples of PNIPAM (5 and 10 wt %) and all additives

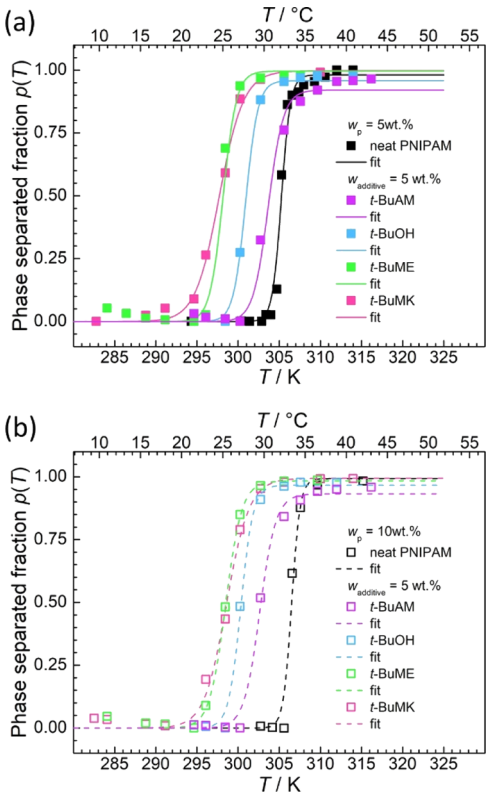

Figure 5. Influence of additive types ($w_{additive}$ = 5 wt %) on the phase-separated fraction $p(T)$ of (a) w_p = 5 wt % and (b) w_p = 10 wt % of PNIPAM as obtained from the NCH resonance of PNIPAM. Key: Full/empty squares = experimental points, full/dashed lines = fits according to eq 6.

(5 wt %). It can be seen that the phase separation temperature T_p decreases (for both PNIPAM concentrations), depending on the additive, in the following order: no additive > *t*-BuAM > *t*-BuOH > *t*-BuME > *t*-BuMK.

Figure 6 shows plots of the phase-separated fraction $p(T)$ obtained from NMR data for all measured combinations of PNIPAM (5 and 10 wt %) and additives (0, 2, 5, and 7 wt %). The data were fitted using eq 6. All relevant thermodynamic parameters (T_p, ΔT_{width}, p_{max}, ΔH, and ΔS) are graphically summarized in Figure 7. It can be seen that there are only small differences in all studied parameters for 5 and 10 wt % of PNIPAM. Increasing the content of any additive decreases the phase separation temperature (T_p, Figure 7a,b), increases the width of phase separation (ΔT_{width}, Figure 7c,d), and decreases both enthalpy (ΔH, Figure 7g,h) and entropy change (ΔS, Figure 7i,j) connected with phase separation of PNIPAM. The

DOI: 10.1021/acsomega.8b01811
ACS Omega 2018, 3, 11865−11873

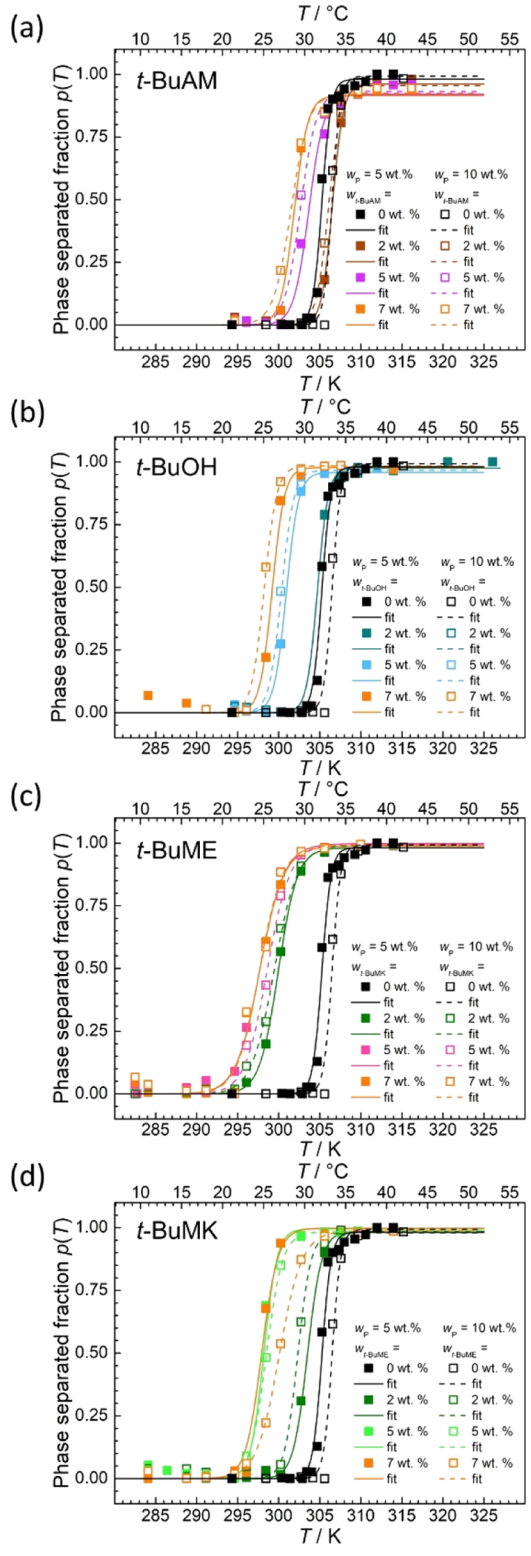

Figure 6. Plots of phase-separated fraction $p(T)$ as obtained from NCH resonances of PNIPAM (solid line 5 wt %; dashed line 10 wt %) with various concentrations of (a) *t*-BuAM, (b) *t*-BuOH, (c) *t*-BuME, and (d) *t*-BuMK. Key: Full/empty squares = experimental points, full/dashed lines = fits according to eq 6.

value of T_p depends on the additive type and decreases in the following order (at constant $w_{additive}$): *t*-BuAM > *t*-BuOH > *t*-BuME > *t*-BuMK. *t*-BuMK has the greatest effect on T_p (decrease of ca. 10 °C), ΔT_{width}, ΔH, and ΔS, which will be discussed in detail later. Values of p_{max} are close to 1 (within experimental error) for all additives (Figure 7e,f).

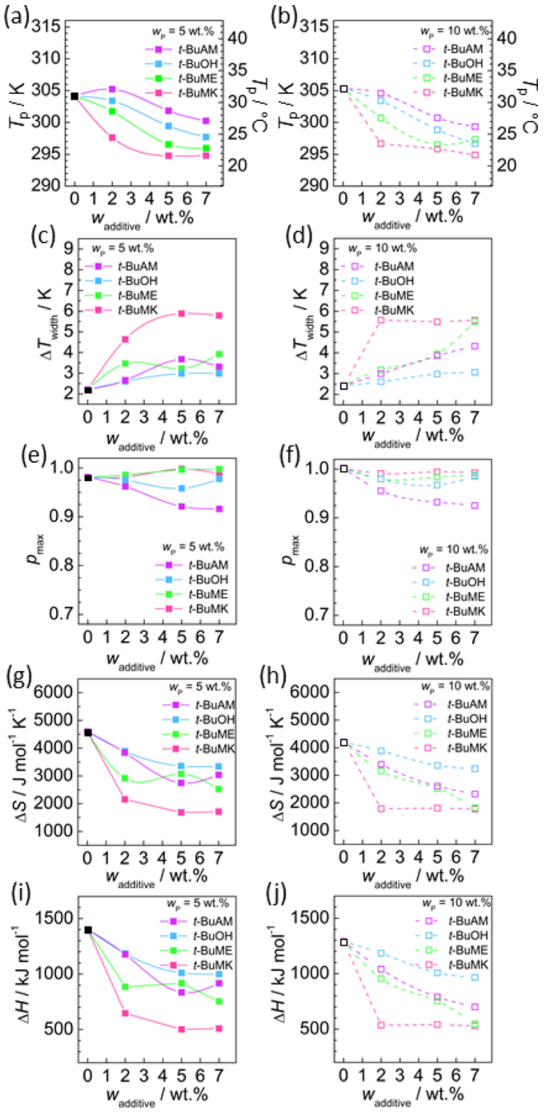

Figure 7. Parameters characterizing phase separation of PNIPAM (5 and 10 wt %) in the presence of the additives studied as denoted in each panel. (a,b) Phase separation temperatures T_p. (c,d) Width of phase separation ΔT_{width}. (e,f) Maximum fraction of phase-separated PNIPAM units p_{max}. (g,h) Variations in standard enthalpy, ΔH. (i,j) Variations in standard entropy, ΔS. Key: Solid and empty black squares correspond to 5 and 10 wt % PNIPAM solutions without additives, respectively.

The additives can be ordered in terms of relative hydrophobicity. Using the values of partition coefficients, log *P* (given in brackets for each additive) estimated using HSPiP software[45] gives the order from least to most hydrophobic additives in the following sequence: *t*-BuAM (0.3) > *t*-BuOH (0.5) > *t*-BuME (0.9) > *t*-BuMK (1.2). From this perspective, the phase separation of PNIPAM is mostly affected by *t*-BuMK because of its hydrophobic association with PNIPAM. This association leads to the partial removal of water molecules from the vicinity of the polymer chains. This effect lowers T_p and ΔH because less heat is required to break hydrogen bonds between polymer chains and solvating water molecules.

Acidity/basicity is another parameter characterizing these additives. Figure 8 is a plot of T_p as a function of pK_a for each

DOI: 10.1021/acsomega.8b01811
ACS Omega 2018, 3, 11865−11873

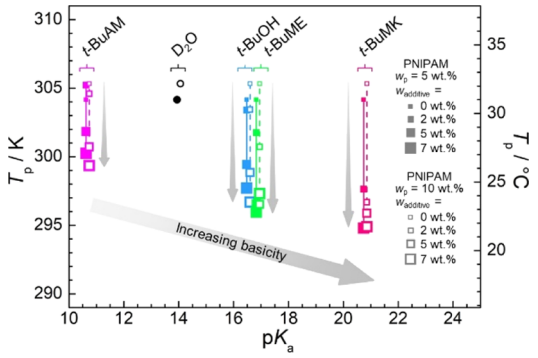

Figure 8. Plot of the phase separation temperature T_p (data from Figure 7a,b) as a function of pK_a of additives and its content ($w_{additive}$) for both 5 and 10 wt % of PNIPAM. The values of pK_a correspond to nondeuterated additives: *t*-BuAM (pK_a = 10.68),[46] *t*-BuOH (pK_a = 16.54),[47] *t*-BuME (pK_a = 16.89),[48] and *t*-BuMK (pK_a = 20.8).[49] The value of pK_a for neat D_2O is set to 14 (same as H_2O) for consistency with additives. For clarity, there are slight offsets of additive pK_a values for 5 and 10 wt % of PNIPAM. All values of pK_a (in H_2O) can be converted to pK_a^* (in D_2O) using the approximate formula pK_a^* = 1.076 × pK_a − 0.45.[50] However, this corresponds practically to a ca. +0.8 pK_a unit shift (i.e., to more basic) of the experimental points, and so it does not change the character of the plot.

additive and its weight fraction. It can be seen that higher pK_a (higher basicity) of the additive lowers T_p. Also, larger content of the same additive decreases the T_p value (vertical gray arrows in Figure 8). This is again because of the higher basicity of the solution. Therefore, pH of the aqueous solution significantly affects the phase separation temperature of PNIPAM.

A series of time-resolved spin−spin ^{1}H NMR relaxation experiments was performed in order to determine the mobilities of water and additive molecules below and above the phase separation temperature of PNIPAM (for w_p = 5 wt %). The values of spin−spin ^{1}H NMR relaxation time T_2 were acquired for residual HDO and also for the *t*-butyl proton resonances of *t*-BuOH, *t*-BuME, and *t*-BuMK as shown in Figure 9. T_2 relaxation times above phase separation (T = 310 K = 37 °C) were significantly shorter than those at the temperature (T = 286 K = 13 °C) below separation for both HDO and *t*-butyl $(CH_3)_3$ groups. This shows that HDO molecules as well as additive molecules exhibit a lower, spatially restricted mobility. Contributions due to chemical exchange[16] are also important because the mobility-restricted solvent molecules are bound within mesoglobules and thus have a low T_2 value. The overall T_2 value is the weighted harmonic mean of bound and free T_2 values, resulting in low overall T_2 above phase separation.[51] The sample was then kept in the NMR magnet at an elevated temperature (T = 310 K = 37 °C), and the time dependence of T_2 was measured. After the value of T_2 had reached a plateau, we observed no further changes of T_2 values over the course of days (Figure 9a−f). T_2 values remained relatively low (ca. 0.7 s for HDO and ca. 0.2 s for *t*-butyl groups of additives), indicating that the solvent molecules remain restricted in mobility and bound in mesoglobular structures. This further indicates that these systems are colloidally stable solutions, such that the phase-separated particles do not aggregate and precipitate. This observation is in contrast to the pristine PNIPAM/D_2O system lacking any additive in which the T_2 relaxation time after 130 h (5.5 days) recovers to its original value (Figure 9g).[10] This

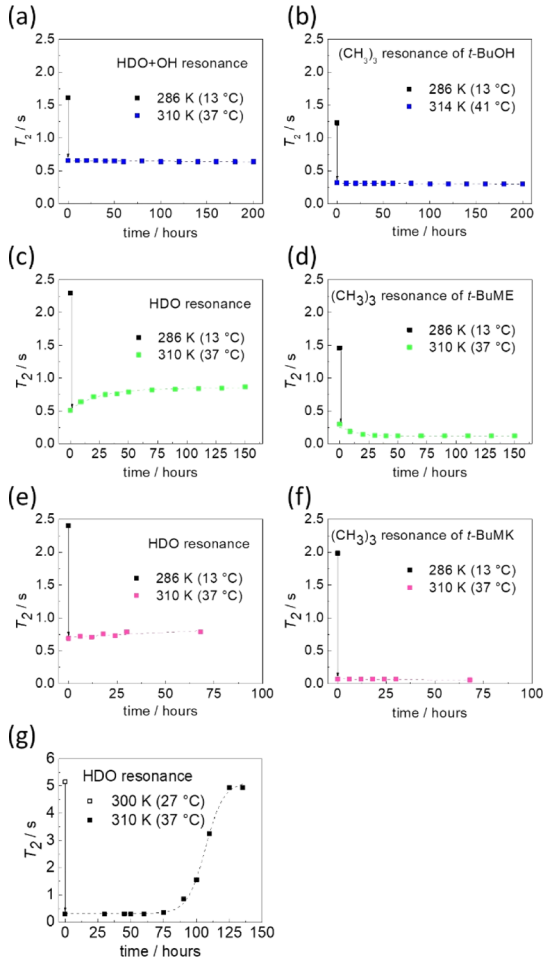

Figure 9. Time dependency of spin−spin relaxation time T_2 of HDO and $(CH_3)_3$ resonances of additives ($w_{additive}$ = 5 wt %) below (T = 286 K = 13 °C) and above (T = 310 K = 37 °C) the phase separation temperature of PNIPAM (w_p = 5 wt %). T_2 values measured in the presence of (a,b) *t*-BuOH, (c,d) *t*-BuME, and (e,f) *t*-BuMK. (g) Pristine PNIPAM/D_2O system (w_p = 5 wt %). Data are taken from ref 10.

corresponds to a state in which water, originally bound in mesoglobules, is very slowly released from these structures, making them more compact. Our observations indicate that the hydrophobic association of PNIPAM and the studied additive molecules increases the colloidal stability of phase-separated polymers sequestering the solvent molecules (both D_2O and the additive) within the mesoglobular structure for extended periods (for at least 8 days in the case of *t*-BuOH). It seems that after phase separation, the additive (which hydrophobically associates with PNIPAM) acts as a shell around the mesoglobules with effective steric stabilizing properties,[4] which prevents further aggregation and precipitation.

DLS data provide information about the size of PNIPAM globules in the presence of additives (*t*-BuAM, *t*-BuOH, *t*-BuME, or *t*-BuMK). There is no significant variation in the hydrodynamic diameters (∼230 nm) for *t*-BuAM, *t*-BuOH, and *t*-BuMK additives (Figure 10a). There is a relatively narrow distribution for *t*-BuAM, which might be caused by its Brønsted-type base character (capability of accepting protons), resulting in a different association mode with PNIPAM. For *t*-BuME additive, it was found that the particle size was smaller

DOI: 10.1021/acsomega.8b01811
ACS Omega 2018, 3, 11865−11873

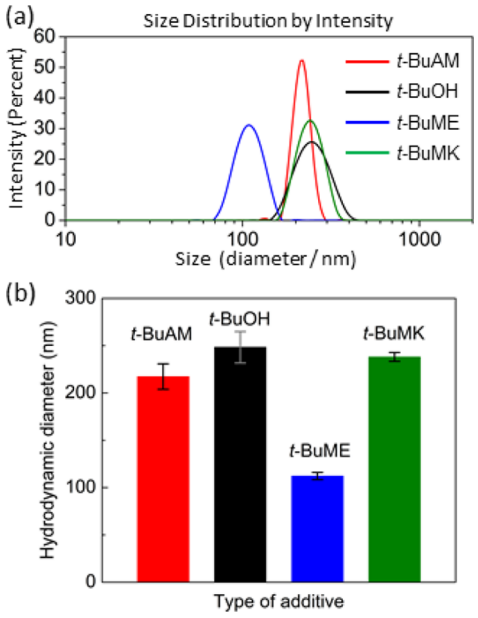

Figure 10. (a) Distribution of hydrodynamic diameters of PNIPAM (w_p = 0.015 wt %, D_2O) with *t*-BuAM, *t*-BuOH, *t*-BuME, or *t*-BuMK ($w_{additive}$ = 5 wt % for all additives) measured at 50 °C. (b) Plot of average values of hydrodynamic diameters.

at around 110 nm in diameter (Figure 10b). This does not correlate with any additive property parameter such as hydrophobicity (log *P*) or acidity (pK_a) and is probably caused by some specific structure-related intermolecular interactions between PNIPAM and *t*-BuME.

3. CONCLUSIONS

In summary, we have reported the effect of low-molecular weight additives, such as *t*-BuAM, *t*-BuOH, *t*-BuME, or *t*-BuMK, on the phase behavior of the PNIPAM polymer in D_2O solutions using NMR and DLS methods. Phase separation was modeled as a two-state process. NMR data were rationalized in terms of a modified van't Hoff equation fitted to the experimental data. This allowed us to obtain accurate values of phase separation temperatures T_p and thermodynamic parameters, such as variations in enthalpy and entropy connected with the phase separation of PNIPAM. We have found that (depending on the additive type) the phase separation temperature T_p decreases (at a constant additive weight fraction) in the following order: T_p(*t*-BuAM) > T_p(*t*-BuOH) > T_p(*t*-BuME) > T_p(*t*-BuMK). T_p also decreases with an increasing concentration of additives. This effect is strongest for *t*-BuMK with a T_p decrease of ca. 10 °C relative to the pristine PNIPAM/D_2O system. We found that the additives hydrophobically associate with the PNIPAM chain, leading to the removal of water molecules from the solvating shell of polymers, thus lowering the enthalpy change of phase separation. An interesting correlation between the pK_a of additives and the phase separation temperature T_p of PNIPAM, that higher pK_a (i.e., higher basicity) leads to lower T_p, was also found. Time-resolved ^{1}H NMR spin−spin relaxation experiments (T_2) above the phase separation temperature revealed that when PNIPAM is in a mesoglobular state, there is no change in the restricted mobility of solvent molecules over the course of days. This indicates the high colloidal stability of phase-separated polymers, with trapping of the solvent molecules (both D_2O and additives) within its structure. This effect is in contrast to the PNIPAM/D_2O system lacking additives in which the majority of water is released from mesoglobules within 5 days. Therefore, a small quantity of a suitable additive can be used for the tuning of PNIPAM properties, such as phase separation temperature, colloidal stability, and morphology/dimensions of formed mesoglobules. Improvements in the stabilities of colloidal solutions of PNIPAM or similar polymers ought also to improve their attractiveness for various applications either simply because of possibilities for extending the stable shelf lives of preparations or because of the tunability of phase separation properties within the physiologically important temperature range.

4. MATERIALS AND METHODS

PNIPAM (M_w = 19 000−26 000 g/mol) (see Figure 1 for the structure) was purchased from Sigma-Aldrich. D_2O (Sigma-Aldrich, 99.9% of deuterium) was used for sample preparation. *tert*-Butyl alcohol (*t*-BuOH), *tert*-butylamine (*t*-BuAM), *tert*-butyl methyl ether (*t*-BuME), and *tert*-butyl methyl ketone (*t*-BuMK) (see Figure 1 for the structures) were purchased from Sigma-Aldrich and used as received. All samples were sealed in 5 mm NMR tubes. The weight fraction of PNIPAM in the binary solvent D_2O/additive was calculated as $w_p = m_p/(m_p + m_{D_2O} + m_{additive}) \times 100\%$ (in wt %), where m_p, m_{D_2O}, and $m_{additive}$ are masses of the PNIPAM polymer, D_2O, and additives, respectively. The composition of the binary solvent D_2O/additive was determined by the weight fraction of an additive in D_2O/additive solution as $w_{additive} = m_{additive}/(m_{D_2O} + m_{additive}) \times 100\%$ (in wt %).

High-resolution ^{1}H NMR spectra were recorded using a Bruker AVANCE III 600 spectrometer operating at 600.2 MHz. During measurements at different temperatures, receiver gain was kept constant to obtain comparable values of integrated intensities. The ^{1}H spin−spin relaxation times T_2 were measured using a CPMG pulse sequence of $90x^\circ - (t_d - 180y^\circ - t_d)_n$—acquisition with a half-echo time t_d = 5 ms. Each experiment was performed over 4 scans with a relaxation delay between scans of 120 s. The resulting T_2 relaxation curves are monoexponential. The fitting process made it possible to determine consistently a single value of the relaxation time. The relative error of T_2 values of the HDO and the additive $(CH_3)_3$ groups did not exceed ±8%. During measurement, temperature was maintained constant within ±0.2 K using a BVT 3000 temperature unit. Prior to each measurement, samples were equilibrated for about 15 min at the measurement temperature.

The hydrodynamic diameter D_h (*z*-average) and size distribution of polymer assemblies in deuterated water (D_2O) (w_p = 0.015 wt %) were determined at 50 °C using a ZEN 3600 Zetasizer Nano Instrument (Malvern Instruments, Malvern, UK). The data were subsequently analyzed using the supplied Malvern Instruments software. Prior to measurement, samples were filtered using a 0.22 μm polyvinylidene fluoride filter to remove any interfering dust particles. Each measurement consisted of an average of five scans.

AUTHOR INFORMATION

Corresponding Authors

*E-mail: Jonathan.Hill@nims.go.jp. Phone: +81-29-860-4578 (J.P.H.).

DOI: 10.1021/acsomega.8b01811
ACS Omega 2018, 3, 11865−11873

*E-mail: Labuta.Jan@nims.go.jp (J.L.).

ORCID

Jonathan P. Hill: 0000-0002-4229-5842

Jan Labuta: 0000-0002-8329-0634

Notes

The authors declare no competing financial interest.

■ ACKNOWLEDGMENTS

This work was supported by the World Premier International Research Initiative (WPI Initiative), the Ministry of Education, Culture, Sports, Science and Technology (MEXT), Japan. The authors also acknowledge Charles University, Prague, Czech Republic, for the support given to N. V. during doctoral studies.

■ ADDITIONAL NOTE

[a]Comparison of exact numerical solution of eq 7 (T_i^{exact}) with approximate solution described by eq 11 (T_i^{approx}) shows that for $\Delta H \geq 10^5$ J mol^{-1} and $\Delta S \geq 200$ J mol^{-1} K^{-1}, the error is $|T_i^{exact} - T_i^{approx}| < 0.04$ K. The lower boundary of ΔH and ΔS is chosen as an extreme case far from experimentally obtained values. For higher values of ΔH and ΔS, the error in determination of T_i using the approximate formula further decreases. Subsequently, errors calculated (using exact and approximate values of T_i) for the phase separation temperature [T_p; eq 12] and the width of the phase separation [ΔT_{width}; eq 14] are $|T_p^{exact} - T_p^{approx}| < 10^{-4}$ K and $|\Delta T_{width}^{exact} - \Delta T_{width}^{approx}| < 10^{-4}$ K, respectively. Therefore, the approximations used here introduce only negligible errors.

■ REFERENCES

(1) Schmaljohann, D. Thermo- and pH-responsive polymers in drug delivery. *Adv. Drug Delivery Rev.* **2006**, *58*, 1655−1670.

(2) Alarcón, C. d. l. H.; Pennadam, S.; Alexander, C. Stimuli responsive polymers for biomedical applications. *Chem. Soc. Rev.* **2005**, *34*, 276−285.

(3) Cheng, H.; Shen, L.; Wu, C. LLS and FTIR studies on the hysteresis in association and dissociation of poly(*N*-isopropylacrylamide) chains in water. *Macromolecules* **2006**, *39*, 2325−2329.

(4) Aseyev, V. O.; Tenhu, H.; Winnik, F. M. Temperature dependence of the colloidal stability of neutral amphiphilic polymers in water. *Adv. Polym. Sci.* **2006**, *196*, 1−85.

(5) Jochum, F. D.; Theato, P. Temperature- and light-responsive smart polymer materials. *Chem. Soc. Rev.* **2013**, *42*, 7468−7483.

(6) Jeong, B.; Gutowska, A. Lessons from nature: stimuli-responsive polymers and their biomedical applications. *Trends Biotechnol.* **2002**, *20*, 305−311.

(7) Ward, M. A.; Georgiou, T. K. Thermoresponsive polymers for biomedical applications. *Polymers* **2011**, *3*, 1215−1242.

(8) Liu, R.; Fraylich, M.; Saunders, B. R. Thermoresponsive copolymers: from fundamental studies to applications. *Colloid Polym. Sci.* **2009**, *287*, 627−643.

(9) Spěváček, J.; Starovoytova, L.; Hanyková, L.; Kouřilová, H. Polymer-solvent interactions in solutions of thermoresponsive polymers studied by NMR and IR spectroscopy. *Macromol. Symp.* **2008**, *273*, 17−24.

(10) Starovoytova, L.; Spěváček, J. Effect of time on the hydration and temperature-induced phase separation in aqueous polymer solutions. 1H NMR study. *Polymer* **2006**, *47*, 7329−7334.

(11) Spěváček, J.; Dybal, J. Stimuli-responsive polymers in solution investigated by NMR and infrared spectroscopy. *Macromol. Symp.* **2011**, *303*, 17−25.

(12) Spěváček, J.; Dybal, J.; Starovoytova, L.; Zhigunov, A.; Sedláková, Z. Temperature-induced phase separation and hydration in poly(*N*-vinylcaprolactam) aqueous solutions: a study by NMR and IR spectroscopy, SAXS, and quantum-chemical calculations. *Soft Matter* **2012**, *8*, 6110−6119.

(13) Spěváček, J.; Hanyková, L.; Labuta, J. Behavior of water during temperature-induced phase separation in poly(vinyl methyl ether) aqueous solutions. NMR and optical microscopy study. *Macromolecules* **2011**, *7*, 2149−2153.

(14) Kouřilová, H.; Šťastná, J.; Hanyková, L.; Sedláková, Z.; Spěváček, J. ^{1}H NMR study of temperature-induced phase separation in solutions of poly(*N*-isopropylmethacrylamide-*co*-acrylamide) copolymers. *Eur. Polym. J.* **2010**, *46*, 1299−1306.

(15) Kouřilová, H.; Spěváček, J.; Hanyková, L. ^{1}H NMR study of temperature-induced phase transitions in aqueous solutions of poly(*N*-isopropylmethacrylamide)/poly(*N*-vinylcaprolactam) mixtures. *Polym. Bull.* **2013**, *70*, 221−235.

(16) Kouřilová, H.; Hanyková, L.; Spěváček, J. NMR study of phase separation in D_2O/ethanol solutions of poly(*N*-isopropylmethacrylamide) induced by solvent composition and temperature. *Eur. Polym. J.* **2009**, *45*, 2935−2941.

(17) Fujishige, S.; Kubota, K.; Ando, I. Phase transition of aqueous solutions of poly(N-isopropylacrylamide) and poly(N-isopropylmethacrylamide). *J. Phys. Chem.* **1989**, *93*, 3311−3313.

(18) Aseyev, V.; Hietala, S.; Laukkanen, A.; Nuopponen, M.; Confortini, O.; Du Prez, F. E.; Tenhu, H. Mesoglobules of thermoresponsive polymers in dilute aqueous solutions above the LCST. *Polymer* **2005**, *46*, 7118−7131.

(19) Heskins, M.; Guillet, J. E. Solution properties of poly(N-isopropylacrylamide). *J. Macromol. Sci., Part A: Pure Appl. Chem.* **1968**, *2*, 1441−1455.

(20) Monerris, M.; Broglia, M.; Yslas, I.; Barbero, C.; Rivarola, C. Antibacterial polymeric nanocomposites synthesized by *in-situ* photoreduction of silver ions without additives inside biocompatible hydrogel matrices based on *N*-isopropylacrylamide and derivatives. *eXPRESS Polym. Lett.* **2017**, *11*, 946−962.

(21) Brun-Graeppi, A. K. A. S.; Richard, C.; Bessodes, M.; Scherman, D.; Merten, O.-W. Thermoresponsive surfaces for cell culture and enzyme-free cell detachment. *Prog. Polym. Sci.* **2010**, *35*, 1311−1324.

(22) Halperin, A.; Kröger, M.; Winnik, F. M. Poly(N-isopropylacrylamide) Phase Diagrams: Fifty Years of Research. *Angew. Chem., Int. Ed.* **2015**, *54*, 15342−15367.

(23) Hofmann, C. H.; Schönhoff, M. Dynamics and distribution of aromatic model drugs in the phase transition of thermoreversible poly(*N*-isopropylacrylamide) in solution. *Colloid Polym. Sci.* **2012**, *290*, 689−698.

(24) Jadhav, S. A.; Scalarone, D.; Brunella, V.; Ugazio, E.; Sapino, S.; Berlier, G. Thermoresponsive copolymer-grafted SBA-15 porous silica particles for temperature-triggered topical delivery systems. *eXPRESS Polym. Lett.* **2017**, *11*, 96−105.

(25) Wang, Y. M.; Zheng, S. X.; Chang, H. I.; Tsai, H. Y.; Liang, M. Microwave-assisted synthesis of thermo- and pH-responsive antitumor drug carrier through reversible addition-fragmentation chain transfer polymerization. *eXPRESS Polym. Lett.* **2017**, *11*, 293−307.

(26) Gandhi, A.; Paul, A.; Sen, S. O.; Sen, K. K. Studies on thermoresponsive polymers: Phase behaviour, drug delivery and biomedical applications. *Asian J. Pharm. Sci.* **2015**, *10*, 99−107.

(27) Filippov, S. K.; Bogomolova, A.; Kaberov, L.; Velychkivska, N.; Starovoytova, L.; Cernochova, Z.; Rogers, S. E.; Lau, W. M.; Khutoryanskiy, V. V.; Cook, M. T. Internal nanoparticle structure of temperature-responsive self-assembled PNIPAM-*b*-PEG-*b*-PNIPAM triblock copolymers in aqueous solutions: NMR, SANS, and light scattering studies. *Langmuir* **2016**, *32*, 5314−5323.

(28) Starovoytova, L.; Spěváček, J.; Trchová, M. 1H NMR and IR study of temperature-induced phase transition of negatively charged poly(N-isopropylmethacrylamide-co-sodium methacrylate) copolymers in aqueous solutions. *Eur. Polym. J.* **2007**, *43*, 5001−5009.

(29) Philipp, M.; Aleksandrova, R.; Müller, U.; Ostermeyer, M.; Sanctuary, R.; Müller-Buschbaum, P.; Krüger, J. K. Molecular versus macroscopic perspective on the demixing transition of aqueous

DOI: 10.1021/acsomega.8b01811
ACS Omega 2018, 3, 11865−11873

PNIPAM solutions by studying the dual character of the refractive index. *Soft Matter* **2014**, *10*, 7297−7305.
(30) Kujawa, P.; Winnik, F. M. Volumetric Studies of Aqueous Polymer Solutions Using Pressure Perturbation Calorimetry: A New Look at the Temperature-Induced Phase Transition of Poly(N-isopropylacrylamide) in Water and D2O. *Macromolecules* **2001**, *34*, 4130−4135.
(31) Gao, Y.; Yang, J.; Ding, Y.; Ye, X. Effect of urea on phase transition of poly(*N*-isopropylacrylamide) investigated by differential scanning calorimetry. *J. Phys. Chem. B* **2014**, *118*, 9460−9466.
(32) Tiktopulo, E. I.; Uversky, V. N.; Lushchik, V. B.; Klenin, S. I.; Bychkova, V. E.; Ptitsyn, O. B. Domain Coil-Globule Transition in Homopolymers. *Macromolecules* **1995**, *28*, 7519−7524.
(33) Šťastná, J.; Hanyková, L.; Spěváček, J. NMR and DSC study of temperature-induced phase transition in aqueous solutions of poly(*N*-isopropylmethacrylamide-*co*-acrylamide) copolymers. *Colloid Polym. Sci.* **2012**, *290*, 1811−1817.
(34) Shechter, I.; Ramon, O.; Portnaya, I.; Paz, Y.; Livney, Y. D. Microcalorimetric study of the effects of a chaotropic salt, KSCN, on the lower critical solution temperature (LCST) of aqueous poly(*N*-isopropylacrylamide) (PNIPA) solutions. *Macromolecules* **2010**, *43*, 480−487.
(35) Hofmann, C.; Schönhoff, M. Do additives shift the LCST of poly (*N*-isopropylacrylamide) by solvent quality changes or by direct interactions? *Colloid Polym. Sci.* **2009**, *287*, 1369−1376.
(36) Starovoytova, L.; Spěváček, J.; Ilavský, M. 1H NMR study of temperature-induced phase transitions in D2O solutions of poly(N-isopropylmethacrylamide)/poly(N-isopropylacrylamide) mixtures and random copolymers. *Polymer* **2005**, *46*, 677−683.
(37) Zhang, Y.; Furyk, S.; Bergbreiter, D. E.; Cremer, P. S. Specific Ion Effects on the Water Solubility of Macromolecules: PNIPAM and the Hofmeister Series. *J. Am. Chem. Soc.* **2005**, *127*, 14505−14510.
(38) Lee, L.-T.; Cabane, B. Effects of surfactants on thermally collapsed poly(*N*-isopropylacrylamide) macromolecules. *Macromolecules* **1997**, *30*, 6559−6566.
(39) Winnik, F. M.; Ottaviani, M. F.; Bossmann, S. H.; Pan, W.; Garcia-Garibay, M.; Turro, N. J. Cononsolvency of poly(N-isopropylacrylamide): a look at spin-labeled polymers in mixtures of water and tetrahydrofuran. *Macromolecules* **1993**, *26*, 4577−4585.
(40) Pica, A.; Graziano, G. An alternative explanation of the cononsolvency of poly(N-isopropylacrylamide) in water-methanol solutions. *Phys. Chem. Chem. Phys.* **2016**, *18*, 25601−25608.
(41) Velychkivska, N.; Bogomolova, A.; Filippov, S. K.; Starovoytova, L.; Labuta, J. Thermodynamic and kinetic analysis of phase separation of temperature-sensitive poly(vinyl methyl ether) in the presence of hydrophobic *tert*-butyl alcohol. *Colloid Polym. Sci.* **2017**, *295*, 1419−1428.
(42) Labuta, J.; Hill, J. P.; Hanyková, L.; Ishihara, S.; Ariga, K. Probing the micro-phase separation of thermo-responsive amphiphilic polymer in water/ethanol solution. *J. Nanosci. Nanotechnol.* **2010**, *10*, 8408−8416.
(43) Spěváček, J.; Hanyková, L. NMR Study on polymer-solvent interactions during temperature-induced phase separation in aqueous polymer solutions. *Macromol. Symp.* **2007**, *251*, 72−80.
(44) Spěváček, J.; Hanyková, L.; Starovoytova, L. ^{1}H NMR relaxation study of thermotropic phase transition in poly(vinyl methyl ether)/D_2O solutions. *Macromolecules* **2004**, *37*, 7710−7718.
(45) Hansen Solubility Parameters in Practice (HSPiP) software. http://www.pirika.com/NewHP/PirikaE/logP.html (web page accessed on Aug 27, 2018).
(46) Juranić, I. Simple method for the estimation of pK_a of amines. *Croat. Chem. Acta* **2014**, *87*, 343−347.
(47) Reeve, W.; Erikson, C. M.; Aluotto, P. F. A new method for the determination of the relative acidities of alcohols in alcoholic solutions. The nucleophilicities and competitive reactivities of alkoxides and phenoxides. *Can. J. Chem.* **1979**, *57*, 2747−2754.
(48) Arnett, E. M.; Wu, C. Y. Base strengths of some aliphatic ethers in aqueous sulfuric acid. *J. Am. Chem. Soc.* **1962**, *84*, 1680−1684.
(49) Zook, H. D.; Kelly, W. L.; Posey, I. Y. Chemistry of enolates. VI. Acidity scale for ketones. Effect of enolate basicity in elimination reactions of halides. *J. Org. Chem.* **1968**, *33*, 3477−3480.
(50) Krżel, A.; Bal, W. A formula for correlating pK_a values determined in D_2O and H_2O. *J. Inorg. Biochem.* **2004**, *98*, 161−166.
(51) Hanyková, L.; Labuta, J.; Spěváček, J. NMR study of temperature-induced phase separation and polymer-solvent interactions in poly(vinyl methyl ether)/D2O/ethanol solutions. *Polymer* **2006**, *47*, 6107−6116.

DOI: 10.1021/acsomega.8b01811
ACS Omega 2018, 3, 11865−11873